Available online at www.sciencedirect.com

ScienceDirect

Journal of Nutritional Biochemistry 24 (2013) 1889–1910

Journal of Nutritional Biochemistry

High glucose-induced proteome alterations in hepatocytes and its possible relevance to diabetic liver disease

Jing-Yi Chen[a], Hsiu-Chuan Chou[b], You-Hsuan Chen[a], Hong-Lin Chan[a,*]

[a]Institute of Bioinformatics and Structural Biology & Department of Medical Sciences, National Tsing Hua University, Hsinchu, Taiwan
[b]Department of Applied Science, National Hsinchu University of Education, Hsinchu, Taiwan

Received 5 March 2013; received in revised form 16 May 2013; accepted 24 May 2013

Abstract

Hyperglycemia can cause several abnormalities in liver cells, including diabetic liver disease. Previous research has shown that high blood glucose levels can damage liver cells through glycoxidation. However, the detailed molecular mechanisms underlying the effects of high blood glucose on the development of diabetic liver disease have yet to be elucidated. In this study, we cultured a liver cell line (Chang liver cell) in mannitol-balanced 5.5 mM, 25 mM and 100 mM D-glucose media and evaluated protein expression and redox regulation. We identified 141 proteins that showed significant changes in protein expression and 29 proteins that showed significant changes in thiol reactivity, in response to high glucose concentration. Several proteins involved in transcription-control, signal transduction, redox regulation and cytoskeleton regulation showed significant changes in expression, whereas proteins involved in protein folding and gene regulation displayed changes in thiol reactivity. Further analyses of clinical plasma specimens confirmed that the proteins AKAP8L, galectin-3, PGK 1, syntenin-1, Abin 2, aldose reductase, CD63, GRP-78, GST-pi, RXR-gamma, TPI and vimentin showed type 2 diabetic liver disease-dependent alterations. In summary, in this study we used a comprehensive hepatocyte-based proteomic approach to identify changes in protein expression and to identify redox-associated diabetic liver disease markers induced by high glucose concentration. Some of the identified proteins were validated with clinical samples and are presented as potential targets for the prognosis and diagnosis of diabetic liver disease.

Keywords: Glucose proteomics; Redox-proteomics; Liver cells; 2D-DIGE; MALDI-TOF MS

1. Introduction

Hyperglycemia is a common characteristic of diabetes mellitus, with frequent modification of amino groups in proteins by monosaccharides. This reaction modifies the function and structure of proteins through the formation of advanced glycation end-products, and generates reactive oxygen species (ROS) during a process called glycoxidation [1]. The glycated proteins eventually induce intracellular oxidative stress, activate a panel of protein kinases and produce a proinflammatory status by interacting with membrane receptors [2–5]. Excess glucose-induced oxidative stress also encourages diabetic complications to develop, resulting in tissue damage [6]. The liver is the main organ of glucose regulation and metabolism; therefore, it would be beneficial to elucidate the biological effects of hyperglycemia in liver cells. Numerous studies have used human hepatocytes, including Chang's liver cells and HepG2 cells, to study environmental and glucose-induced oxidation in vitro. For example, HepG2 cells cultured at high glucose levels exhibited an up-regulation of the gene expression of the human apolipoprotein A-II gene, which can lead to an increased level of plasma triglyceride and glucose intolerance, causing hyperglycemia [7]. In addition, high glucose levels inhibit 5′AMP-activated protein kinase, which plays a central role in the modulation of cellular energy homeostasis [8]. Furthermore, high concentrations of glucose induced an insulin-resistant condition in HepG2 cells indicated by decreased Akt activity, and its downstream glycogen synthase kinase 3a/b [9]. All of these studies suggest that high glucose concentrations elicit detrimental alterations in liver cells.

Several chemical groups have been identified as potential targets of ROS in cells. One of these, the free thiol group (RSH) of cysteine residues, is a potent nucleophilic agent and is able to undergo a number of redox-induced modifications under physiological conditions. Oxidative modification of RSH groups other than disulphide formation includes the formation of sulfenic acid, sulfinic acid and

Abbreviations: 1-DE, one-dimensional gel electrophoresis; 2-DE, two-dimensional gel electrophoresis; Ab, antibody; CCB, colloidal coomassie blue; CHAPS, 3-[(3-cholamidopropyl)-dimethylammonio]-1-propanesulfonate); ddH_2O, double deionized water; DIGE, differential gel electrophoresis; DTT, dithiothreitol; FCS, fetal calf serum; MALDI-TOF MS, matrix assisted laser desorption ionization-time of flight mass spectrometry; NP-40, Nonidet P-40; TFA, trifluoroacetic acid.

* Corresponding author. Institute of Bioinformatics and Structural Biology & Department of Medical Sciences, National Tsing Hua University, No.101, Kuang-Fu Rd. Sec.2, Hsinchu, 30013, Taiwan. Tel.: +886 3 5742476; fax: +886 3 5715934.

E-mail address: hlchan@life.nthu.edu.tw (H.-L. Chan).

0955-2863/$ - see front matter © 2013 Elsevier Inc. All rights reserved.
http://dx.doi.org/10.1016/j.jnutbio.2013.05.006

sulfonic acid, depending on the oxidative capacity of the oxidant [10]. Oxidation of RSH groups to sulfinic and sulfonic acids is an irreversible reaction under physiological conditions and induces a loss of biological function in proteins [11,12].

Two-dimensional gel electrophoresis (2-DE) is an extensively used proteomic separation technique, used to analyse differentially expressed proteins in biological samples [13–16]. However, 2-DE and the methods regularly used for in-gel protein visualizations are inherently variable, and many replicate gels must be run before significant differences in protein expression can be accurately identified. Additionally, these protein visualization strategies often have narrow linear dynamic ranges of detection, making them unsuitable for the analysis of biological samples where protein copy numbers show large variation. The introduction of 2D-difference gel electrophoresis (2D-DIGE), which can co-detect several biological samples on the same 2-DE gel, thus reducing gel-to-gel variation, has markedly improved gel-based methods of protein quantification and detection [17–21].

We evaluated changes in hepatotic protein expression associated with high glucose concentrations using lysine- and cysteine-labeling 2D-DIGE [22,23]. Combined strategies of matrix-assisted laser desorption ionization-time of flight mass spectrometry (MALDI-TOF MS) and clinical plasma analysis confirmed the changes in protein expression and redox-associated hepatotic markers induced by high glucose concentrations. Our results indicated potential targets for the prognosis and diagnosis of diabetic liver disease. To our knowledge, this is the first study not only to report the effects of high glucose concentrations on global protein expression and redox regulation in hepatocytes, but also to associate these findings with diabetic liver disease.

2. Materials and methods

2.1. Chemicals and reagents

Generic chemicals were purchased from Sigma-Aldrich (St. Louis, MO, USA), while reagents for lysine-2D-DIGE were purchased from GE Healthcare (Uppsala, Sweden). The synthesis of the iodoacetylated cyanine 3 (ICy3) and 5 (ICy5) dyes has been previously reported [24–29]. All primary antibodies were purchased from GeneTex (Hsinchu, Taiwan) as well as anti-mouse, and anti-rabbit secondary antibodies were purchased from GE Healthcare (Uppsala, Sweden). All the chemicals and biochemicals used in this study were of analytical grade.

2.2. Cell lines and cell cultures

The cell line, Chang liver cell, was purchased from the American Type Culture Collection (Manassas, VA, USA) and was maintained in Dulbecco's Modified Eagle's medium supplemented with 10% (v/v) fetal calf serum, L-glutamine (2 mM), streptomycin (100 μg/ml) and penicillin (100 IU/ml) (all from Gibco-Invitrogen, UK). Chang liver cells were incubated at 37°C and 5% CO_2.

For cell culturing at differential glucose concentrations, the cultures were exposed to D-glucose at a final concentration of 25 and 100 mM (corresponding to 2 h after meal plasma glucose level of diabetic patients and glucose level in uncontrolled diabetic patients [30], respectively) and compared with cultures exposed to 5.5 mM D-glucose as control (corresponding to fasting plasma glucose level of diabetes-free people) [31,32]. To exclude the possible effects of hyperosmotic stress, mannitol was used to balance the differential glucose concentrations according to a previous report [33]. After exposure for at least 3 weeks, the monolayer cultures were used for further analysis.

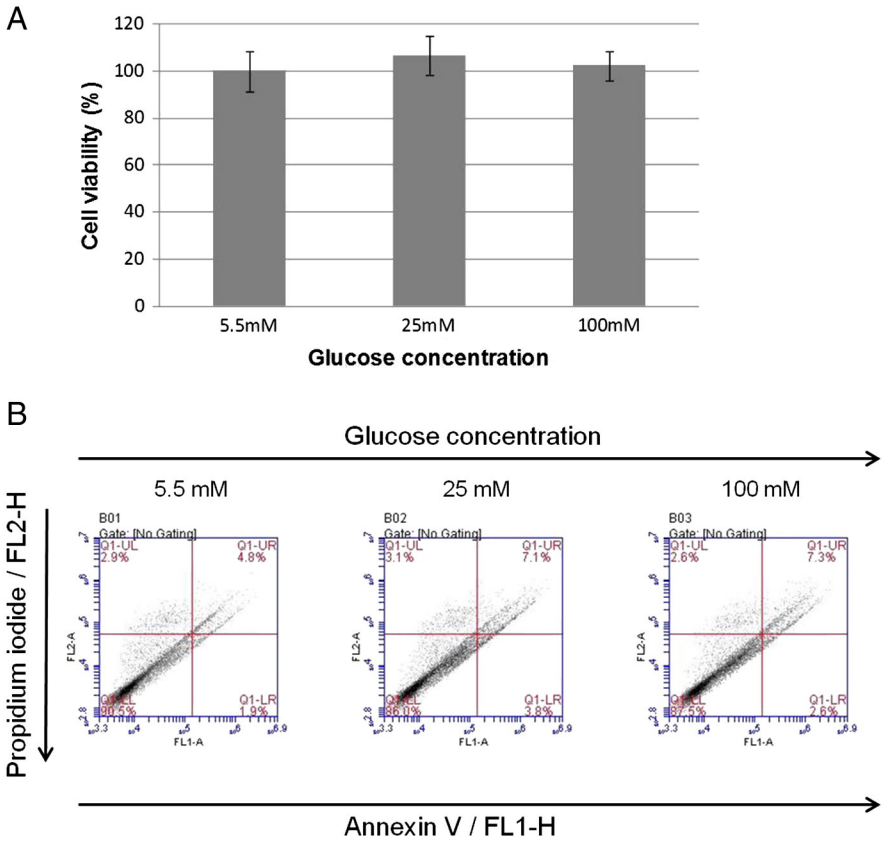

Fig. 1. Effect of glucose concentration on cell viability and cell apoptosis in Chang liver cells. (A) MTT-based viability assays were performed on Chang liver cells cultures following 3 weeks at different glucose concentrations (5.5 mM, 25 mM and 100 mM glucose). Paired Student's *t* test has been used for the statistical analysis of the experimental results. Values were normalized against untreated samples and are the average of three independent measurements +/− the standard deviation. (B) 10^6 different glucose concentrations cultured Chang liver cells were incubated with Alexa Fluor 488 and propidium iodide in 1× binding buffer at room temperature for 15 min, and then stained cells were analyzed by flow cytometry to examine effect of different glucose concentrations on apoptosis in Chang liver cells. Annexin V is presented in *x*-axis as FL1-H, and propidium iodide is presented in *y*-axis as FL2-H. LR quadrant indicates the percentage of early apoptotic cells (Annexin V positive cells), and UR quadrant indicates the percentage of late apoptotic cells (Annexin V positive and propidium iodide positive cells).

2.3. MTT cell viability assay

Chang liver cells maintaining in mannitol-balanced 5.5 mM, 25 mM and 100 mM glucose, respectively, for at least 3 weeks were trypsinized, counted using a haemocytometer and 5,000 cells/well were seeded into 96-well plates. The culture was then incubated in mannitol-balanced 5.5 mM, 25 mM and 100 mM glucose for 24 h followed by removal of the medium. 50 μl of MTT working solution (1 mg/ml) (Sigma) was added to the cells in each well, followed by a further incubation at 37°C for 4 h. The supernatant was carefully removed; 100 μl of DMSO was added to each well and the plates were shaken for 20 min. The absorbance of samples was then measured at a wavelength of 540 nm in a multi-well plate reader. Values were normalized against the untreated samples and were averaged from 8 independent measurements. The statistic comparisons used in this study were performed with two-group paired Student's *t* test.

2.4. Flow cytometry analysis for apoptosis detection

Annexin-V/propidium iodide (PI) double assay was performed using the Annexin V, Alexa Fluor® 488 Conjugate Detection kit (Life technologies). Following Chang liver cells growing in differential glucose concentration media, cells were typsinized from culture dish and washed twice with cold phosphate-buffered saline (PBS). Chang liver cells (10^6) were resuspended in 500 μl binding buffer and stained with 5 μl Alexa Fluor 488 conjugated annexin V according to the manufacturer's instructions. 1 μl 100μg/ml PI was added and mixed gently to incubate with cells for 15 min at room temperature in the dark. After incubation period, samples were subjected to flow cytometry analysis in 1 h using BD Accuri C6 Flow Cytometry (BD Biosciences, San Jose, CA, USA). The data were analyzed using Accuri CFlow® and CFlow Plus analysis software (BD Biosciences).

2.5. Assay for endogenous reactive oxygen species using 2,7-dichlorofluorescin diacetate (DCFH-DA)

Chang liver cells maintaining in mannitol-balanced 5.5 mM, 25 mM and 100 mM glucose, respectively, for at least 3 weeks were trypsinized, counted using a haemocytometer and 10,000 cells/well were seeded into multiple 24-well plates. The culture was then incubated in mannitol-balanced 5.5 mM, 25 mM and 100 mM glucose for 24 h. After two washes with PBS, cells were treated with 10 μM of 2,7-dichlorofluorescin diacetate (DCFH-DA; Molecular Probes) at 37°C for 20 min and subsequently washed with PBS. Fluorescence was recorded at an excitation wavelength 485 nm and emission wavelength at 530 nm. The statistic comparisons used in this study were performed with two group paired Student's *t* test.

2.6. Sample preparation for 2D-DIGE and gel image analysis

For expression 2D-DIGE, protein samples were labeled with *N*-hydroxysuccinimidyl ester-derivatives of the cyanine dyes Cy2, Cy3 and Cy5 following the protocol described previously [34,35]. Briefly, 150 μg of protein sample was minimally labeled with 375 pmol of either Cy3 or Cy5 for comparison on the same 2-DE. To facilitate image matching and cross-gel statistical comparison, a pool of all samples was also prepared and labeled with Cy2 at a molar ratio of 2.5 pmol Cy2 per μg of protein as an internal standard for all gels. Thus, the triplicate samples and the internal standard could be run and quantified over multiple 2-DE gels. Afterward, image analysis was performed using DeCyder 2-D Differential Analysis Software v7.0 (GE Healthcare) to co-detect, normalize and quantify the protein features in the images. Features detected from non-protein sources (e.g. dust particles and dirty backgrounds) were filtered out. Spots displayed in all five gel images (three images per gel) with a (≥1.3-fold or greater average increase or decrease in abundance ($P < .05$) were considered significant for protein identification.

For redox DIGE analysis, cells were lysed in 2-DE buffer (4% w/v CHAPS, 8 M urea, 10 mM Tris–HCl pH 8.3 and 1 mM EDTA) in the presence of ICy3 or ICy5 (80 pmol/mg protein) on ice to limit post-lysis thiol modification. Proteins from 5.5/25 mM glucose cultured Chang liver cells were labeled with the ICy5 dye and mixed with an equal amount of a standard pool of both samples labeled with ICy3. Since ICy dyes interfered with the protein assay, protein concentrations were determined on replica lysates not containing dye. Lysates were left in the dark for 1 h followed by labeling with Cy2 to monitor protein level. The reactions were quenched with dithiothreitol (DTT) (65 mM final concentration) for 10 min followed by L-lysine (20-fold molar ratio excess of free L-lysine to Cy2 dye) for a further 10 min. Volumes were adjusted to 450 μl with buffer plus DTT and immobilized pH gradient (IPG) buffer for rehydration. All samples were run in triplicate against the standard pool.

2.7. Protein staining, in-gel digestion, and MALDI-TOF MS analysis

Colloidal coomassie blue G-250 staining was used to visualize CyDye-labeled protein features in 2-DE gels followed by excised post-stained gel sections for identification by MALDI-TOF MS. The detailed procedures for protein staining, in-gel digestion and MALDI-TOF MS analysis, together with the algorithm used for data processing were described in our previous publication [19]. The spectrometer was calibrated with a peptide calibration standard (Bruker Daltonics), and internal calibration was performed using the trypsin autolysis peaks at *m/z* 842.51 and *m/z* 2211.10. Peaks in the mass range of *m/z* 700–3000 were used to generate a peptide mass fingerprint that was searched against in the Swiss-Prot/TrEMBL database (released on 2011_08) with 531473 entries, using Mascot software v2.3.02 (Matrix Science, London, UK). We used the following strings for the search: *Homo sapiens*; tryptic digest with a maximum of 1 missed cleavage; carbamidomethylation of cysteine, partial protein N-terminal acetylation, partial methionine oxidation and partial modification of glutamine to pyroglutamate and a mass tolerance of 50 ppm. Identification was accepted based on significant Mascot Mowse scores ($P<.05$), spectrum annotation and observed versus expected molecular weight and p*I* on 2-DE gels.

2.8. Immunoblotting analysis and enzyme-linked immunosorbent assay (ELISA) analysis

Immunoblotting and ELISA analyses were used to validate the differential abundance of proteins identified by mass spectrometry. The detailed experimental procedures were described in our previous reports [17,36,37]. All primary antibodies used for expression validation were purchased from Genetex (Hsinchu, Taiwan). Plasma samples used for immunoblotting and ELISA analysis were not used to remove albumin and IgG because the analytical tools used were sufficiently sensitive to detect low-abundance proteins in whole plasma. The statistic comparisons used in this study were performed with two-group paired Student's *t* test.

2.9. Plasma sample collection and purification

From Jan to Dec 2009, 20 donors in a single center (Chiayi Christian Hospital, Chiayi, Taiwan) were enrolled into the study. Those included in the study were divided into type 2 diabetes mellitus with liver disease ($n=10$) and healthy donor groups ($n=10$). The criteria to assess the presence of type 2 diabetes mellitus were based on the guidelines proposed by the World Health Organization. All type 2 diabetic patients had typical diabetic symptoms along with a single fasting plasma glucose level of >7 mM or 2 h postprandial plasma glucose level of >11.1 mM. Healthy individuals with their fasting blood glucose below 5.5 mM were selected as controls. This study was approved by the Institutional Research Board and carried out according to the Helsinki Declaration Principles. Written informed consent was collected from all participating subjects.

3. Results

3.1. High glucose concentration induces changes in protein expression in the Chang liver cells

To evaluate the effects of high glucose concentration on the expression of hepatocyte proteins, we cultured Chang liver cells in mannitol-balanced 5.5 mM, 25 mM, and 100 mM glucose media for at least 3 weeks. We then performed MTT and apoptotic assays. Our results indicated that the Chang liver cells showed insignificant variation in viability and apoptosis among the three culture conditions (Figs. 1A and B). We evaluated protein expression in the Chang liver cells and identified 1939 protein spots and 279 protein features that displayed differential expression among the three conditions (≥1.3-fold changes; $P<0.05$). We used MALDI-TOF MS to identify proteins in 141 of these features (Table 1, Figs. 2 and 3). The differentially expressed proteins were predominantly located in the cytoplasm, nucleus, and secreted fraction. Their functions included transcription control, signal transduction, redox regulation, and cytoskeleton regulation (Fig. 4 and Table 1).

To further verify the up-regulation or down-regulation of the identified proteins, we performed immunoblot and ELISA analyses of proteins modulated by high glucose concentrations (25 mM and 100 mM), and compared them with proteins in control cells (5.5 mM glucose) (Fig. 5). We used specific antibodies against Abin 2, AKAP-9, Annexin 5, Copine-9, FUCA2, Galectin-3, GRP 78, GSTP1, IGFBP2, IGFBP4, L-plastin, Lamin A/C, MPR, PDI, PGK 1, PI-TP-β, Prx-6, RSK2, RXR-γ, Syntenin-1 and Vimentin, as illustrated in Fig. 5. 2D-DIGE analysis provided further evidence of changes in protein expression in response to glucose treatment (Table 1).

3.2. Clinical validation of findings using diabetic plasma specimens

We analyzed diabetic plasma specimens using immunoblotting and ELISA to confirm the clinical relevance of the findings of the

Table 1
Alphabetic list of identified differentially expressed proteins after 2D-DIGE coupled with MALDI-TOF mass spectrometry analysis of Chang liver cells maintained in mannitol-balanced 5.5 mM, 25 mM and 100 mM glucose

No.	Swiss-prot No.	Protein name	pI	MW	Coverage (%)	No. Match. Peptides	Score	Subcellular location	Functional ontology	Ratio (25mM/5.5mM)	*P*-value	Ratio (100mM/5.5mM)	*P*-value
1433	P31946	14-3-3 protein beta/alpha	4.76	28181	36	10/16	124/56	Cytoplasm	Signal transduction	1.19	0.069	1.51	.0006
1307	Q7M4R4	14-3-3 protein epsilon/14-3-3E	4.63	29326	53	16/48	115/56	Cytoplasm	Signal transduction	1.37	0.003	−1.20	.015
1402	P61981	14-3-3 protein gamma	4.80	28456	30	10/26	78/56	Cytoplasm	Signal transduction	1.33	0.0017	−1.13	.019
1367	P61981	14-3-3 protein gamma	4.80	28456	27	9/34	72/56	Cytoplasm	Signal transduction	1.30	0.0055	−1.20	.0065
1365	Q6NUR9	14-3-3 protein zeta/delta	4.73	27899	66	20/58	152/56	Cytoplasm	Signal transduction	1.40	0.0044	−1.17	.014
262	P11021	78 kDa glucose-regulated protein/GRP-78	5.07	72402	42	27/47	231/56	ER	Protein folding	−1.24	0.24	−1.95	.0039
287	P11021	78 kDa glucose-regulated protein/GRP-78	5.07	72402	49	34/66	259/56	ER	Protein folding	−1.53	7.80E-06	−1.69	.0011
856	Q96HG5	Actin, cytoplasmic 1	5.29	42052	58	25/68	157/56	Cytoplasm	Cytoskeleton	1.34	.0078	1.63	.00033
838	P63261	Actin, cytoplasmic 2	5.31	42108	54	22/56	145/56	Cytoplasm	Cytoskeleton	1.59	.01	1.75	.0014
797	Q9H0C2	ADP/ATP translocase 4	9.91	35285	17	6/10	79/56	Mitochondrion	Transport	1.16	.14	1.43	.0048
1402	Q99996	A-kinase anchor protein 9/AKAP-9	4.95	455725	7	29/36	72/56	Cytoplasm	Signal transduction	1.33	.0017	−1.13	.019
1130	P52895	Aldo-keto reductase family 1 member C2	7.13	37118	17	8/13	97/56	Cytoplasm	Lipid Metabolism	−1.22	.089	−1.60	.0024
1158	P15121	Aldose reductase/AR	6.51	36230	59	18/80	176/56	Cytoplasm	Redox regulation	1.79	.018	1.54	.0034
1204	P15121	Aldose reductase/AR	6.51	36230	59	18/69	187/56	Cytoplasm	Redox regulation	2.85	.0003	1.77	.002
1207	P15121	Aldose reductase/AR	6.51	36230	68	18/55	228/56	Cytoplasm	Redox regulation	2.20	.00015	1.78	.00023
1214	P15121	Aldose reductase/AR	6.51	36237	16	6/27	71/56	Cytoplasm	Redox regulation	1.99	.0056	1.84	.00067
1069	P51693	Amyloid-like protein 1/APLP-1	5.54	72815	11	12/28	79/56	Plasma membrane	Signal transduction	1.86	.0073	1.21	.1
1687	Q86XL3	Ankyrin repeat and LEM domain containing protein 2	6.66	104905	7	7/12	60/56	ER	Mitosis	1.15	.16	1.51	.0058
1348	Q86XL3	Ankyrin repeat and LEM domain containing protein 2	6.66	104905	6	7/31	56/56	ER	Mitosis	1.82	.0025	−1.05	.2
311	P09525	Annexin A4	5.84	36088	23	7/22	64/56	Plasma membrane	Calcium regulation	−1.25	.12	1.24	.00099
1288	P08758	Annexin A5	4.94	35971	17	6/17	80/56	Plasma membrane	Calcium regulation	−1.63	.039	−1.01	.93
1115	P53004	Biliverdin reductase A/BVR A	6.06	33692	32	9/35	112/56	Cytoplasm	Redox regulation	−1.06	.68	−1.51	.017
716	P07339	Cathepsin D	6.10	45037	21	9/19	95/56	Lysosome	Protein degradation	1.29	.11	1.61	.0088
412	P08962	CD63 antigen	8.14	26474	23	7/33	62/56	Plasma membrane	Growth regulation	−1.55	.17	1.11	.43
302	Q96ST8	Centrosomal protein of 89 kDa	6.36	89934	16	13/33	61/56	Cytoplasm	Cytoskeleton regulation	−1.68	.0005	1.13	.2
1194	Q96L14	Cep170-like protein	5.45	32628	15	3/5	59/56	Cytoplasm	Cytoskeleton regulation	1.49	.025	1.86	.0046
1628	Q14406	Chorionic somatomammotropin hormone-like 1	5.55	25660	14	4/10	58/56	Secreted	Hormone	1.48	.012	1.09	.41
1678	Q14406	Chorionic somatomammotropin hormone-like 1	5.55	25660	12	4/9	57/56	Secreted	Hormone	1.5	.057	1.76	.099
1673	P23528	Cofilin-1	8.22	18719	31	5/15	63/56	Cytoplasm	Cytoskeleton regulation	2.14	5.30E-06	2.15	.00044
59	Q9H2F9	Coiled-coil domain-containing protein 68	8.78	39073	21	6/13	67/56	Cytoplasm	unknown	1.31	.3	1.68	.0069
929	Q8IYJ1	Copine-9	5.18	62281	15	7/27	57/56	Cytoplasm	Vesicle transport	1.83	.00064	1.11	.27
1867	P62937	Cyclophilin A/Peptidyl-prolyl cis-trans isomerase A/PPIase A	7.68	18229	31	7/16	70/56	Cytoplasm	Mitosis	1.50	.0064	1.12	.21
1571	Q96Q81	Deoxyuridine 5′-triphosphate nucleotidohydrolase	9.65	26975	28	6/24	64/56	Cytoplasm	Protein folding	1.42	.4	1.42	.051
1753	Q96Q81	Deoxyuridine 5′-triphosphate nucleotidohydrolase, mitochondrial/dUTPase	9.46	26832	43	9/20	95/56	Mitochondrion	Nucleotide metabolism	−1.08	.8	−1.69	.049
442	Q5KSL6	Diacylglycerol kinase kappa/DAG kinase kappa	5.36	143678	18	22/71	64/56	Plasma membrane	Signal transduction	−2.19	.008	1.03	.8
704	Q13115	Dual specificity protein phosphatase 4	7.10	43781	10	5/5	56/56	Nucleus	Signal transduction	1.47	.058	1.21	.98
373	Q12805	EGF-containing fibulin-like extracellular matrix protein 1	4.95	56885	26	11/56	110/56	Secreted	Signal transduction	−1.65	.13	1.23	.25

Table 1 (*continued*)

No.	Swiss-prot No.	Protein name	pI	MW	Coverage (%)	No. Match. Peptides	Score	Subcellular location	Functional ontology	Ratio (25mM/5.5mM)	*P*-value	Ratio (100mM/5.5mM)	*P*-value
1173	Q9NQ30	Endothelial cell-specific molecule 1	7.37	21108	19	4/4	60/56	Secreted	Cell growth	1.7	.15	−1.5	.18
1969	Q587J8	ES cell-associated transcript 1 protein	9.47	24291	23	5/12	61/56	Cytoplasm	Mitosis	−1.47	.51	1.17	.47
34	A6NMX2	Eukaryotic translation initiation factor 4E type 1B	6.68	27750	19	5/15	56/56	Cytoplasm	Translation control	2.80	NA	4.53	.0019
1831	P63241	Eukaryotic translation initiation factor 5A-1	5.08	17049	63	11/37	96/56	Cytoplasm	Translation control	−1.53	0.0046	−1.88	.00034
1071	Q96CN4	EVI5-like protein	5.25	91832	8	7/13	56/56	Cytoplasm	Vesicle transport	1.26	.17	2.11	.00091
1216	P52907	F-actin-capping protein subunit alpha-1	5.45	33073	28	8/27	77/56	Cytoplasm	Cytoskeleton regulation	1.26	.061	1.58	.013
1648	O60258	Fibroblast growth factor 17	10.43	25164	20	4/7	56/56	Secreted	Growth factor	1.48	.012	1.09	.41
36	P04075	Fructose-bisphosphate aldolase A	8.30	39851	9	4/11	58/56	Cytoplasm	Glycolysis	1.87	.006	3.02	.00045
1090	P04075	Fructose-bisphosphate aldolase A	8.30	39851	59	19/64	206/56	Cytoplasm	Glycolysis	1.60	.00074	1.33	.013
1004	P17931	Galectin-3	8.57	26193	28	6/25	70/56	Secreted	Immuno response	1.27	.39	2.15	.055
911	Q9NXN4	Ganglioside-induced differentiationassociated protein 2	5.68	56589	9	6/14	62/56	Mitochondrion	Signal transduction	1.11	.36	1.32	.054
1455	P21266	Glutathione S-transferase Mu 3/hGSTM3-3	5.37	26998	47	14/38	131/56	Cytoplasm	Redox regulation	1.10	.43	−1.83	.00028
1499	P09211	Glutathione S-transferase P	5.43	23569	57	13/35	127/56	Cytoplasm	Redox regulation	1.72	.00088	1.37	.0017
446	O43390	Heterogeneous nuclear ribonucleoprotein/hnRNP R	8.35	71184	12	9/18	63/56	Nucleus	Transcription control	−2.09	.00032	1.02	.77
702	Q16576	Histone-binding protein RBBP7	4.89	48132	24	12/34	91/56	Nucleus	Transcription control	1.52	.0072	1.30	.012
863	A6NJ69	IgA-inducing protein homolog	9.13	6161	30	3/13	56/56	Secreted	Immuno response	1.1	.65	2.3	.18
1257	P22692	Insulin-like growth factor-binding protein 4/IBP-4	6.81	29113	39	12/43	109/56	Secreted	Signal transduction	1.30	.12	1.64	.015
1261	Q16270	Insulin-like growth factor-binding protein 7	8.25	30138	52	15/57	154/56	Secreted	Signal transduction	1.71	.026	1.67	.0088
1200	Q16270	Insulin-like growth factor-binding protein 7	8.25	30138	36	13/33	143/56	Secreted	Signal transduction	1.51	.0046	1.90	.0044
452	Q14145	Kelch-like ECH-associated protein 1	6.00	71160	15	9/43	56/56	Cytoplasm	Transcription control	−2.00	NA	1.06	NA
1501	Q9NZU5	LIM and cysteine-rich domains protein 1	8.27	42004	22	6/10	69/56	Cytoplasm	Glycolysis	1.42	.00072	1.64	.015
1261	P00338	L-lactate dehydrogenase A chain/LDH-A	8.44	36950	27	10/37	89/56	Nucleus	Transcription control	1.71	.026	1.67	.0088
1341	O00264	Membrane-associated progesterone receptor component 1/MPR	4.56	21772	15	4/10	57/56	Plasma membrane	Signal transduction	1.57	.004	1.36	.012
207	Q96T33	Merlin	6.11	69874	22	10/43	61/56	Cytoplasm	Growth suppression	−1.98	.0052	1.12	.14
1489	Q5JR59	Microtubule-associated tumor suppressor candidate 2	6.23	150901	6	11/24	62/56	Cytoplasm	Cytoskeleton regulation	−1.88	.00004	−1.10	.00023
1547	Q9Y6H3	Mitochondrial inner membrane protease ATP23 homolog	8.30	28690	28	7/31	60/56	Mitochondrion	Protein degradation	1.44	.0022	−1.09	.46
1226	Q9BWK5	Modulator of retrovirus infection homolog	5.16	17046	19	6/18	81/56	Cytoplasm	Protein degradation	1.41	.3	1.12	.53
158	Q96EN8	Molybdenum cofactor sulfurase	6.23	99084	9	7/16	57/56	Cytoplasm	Metabolism	1.01	.98	1.53	.027
295	Q9UI09	NADH dehydrogenase [ubiquinone] 1 alpha subcomplex subunit 12	9.63	17104	34	5/18	64/56	Mitochondrion	Electron transport	−1.59	.0014	1.16	.018
388	O43678	NADH dehydrogenase [ubiquinone] 1 alpha subcomplex subunit 2	9.62	11029	36	5/31	63/56	Mitochondrion	Electron transport	−2.14	.00081	1.04	.63
1025	Q9UL56	NADH-cytochrome b5 reductase 3/B5R	7.18	34445	14	9/6	83/56	Mitochondrion	Electron transport	1.57	.0045	1.04	.66
1855	P13725	Oncostatin-M	10.71	28751	17	7/22	63/56	Secreted	Growth regulation	−1.06	.6	−1.45	.018
376	Q01804	OTU domain-containing protein 4	6.25	124695	8	10/50	65/56	Unknown	Unknown	−1.44	.0066	1.12	.055
929	Q8TEW0	Partitioning defective 3 homolog/PARD-3	7.41	151844	7	11/26	60/56	Plasma membrane	Mitosis	1.83	.00064	1.11	.27
295	O95613	Pericentrin	5.40	380600	5	19/32	59/56	Cytoplasm	Redox regulation	−1.59	.0014	1.16	.018
1583	Q06830	Peroxiredoxin-1	8.27	22324	33	7/23	107/56	Cytoplasm	Redox regulation	1.85	.000033	2.58	.00000054

(*continued on next page*)

Table 1 (*continued*)

No.	Swiss-prot No.	Protein name	pI	MW	Coverage (%)	No. Match. Peptides	Score	Subcellular location	Functional ontology	Ratio (25mM/5.5mM)	*P*-value	Ratio (100mM/5.5mM)	*P*-value
1564	Q06830	Peroxiredoxin-1	8.27	22324	33	8/19	94/56	Cytoplasm	Redox regulation	1.50	.027	1.09	.56
1627	Q06830	Peroxiredoxin-1	8.27	22324	41	10/29	111/56	Cytoplasm	Redox regulation	1.67	.041	1.45	.076
1700	Q06830	Peroxiredoxin-1	8.27	22324	33	7/23	86/56	Cytoplasm	Redox regulation	1.75	.019	1.93	.0053
1467	P30041	Peroxiredoxin-6	6.00	25133	37	10/22	134/56	Cytoplasm	Redox regulation	−2.57	.0002	−2.75	.000012
1183	P30041	Peroxiredoxin-6	6.00	25133	27	6/17	72/56	cytoplasm	Redox regulation	−1.2	.04	−1.32	.014
1273	P48739	Phosphatidylinositol transfer protein beta isoform/ PI-TP-beta	6.41	31810	28	10/26	90/56	Cytoplasm	Transport	1.74	.00091	1.37	.0083
547	P00558	Phosphoglycerate kinase 1	8.30	44985	20	7/14	66/56	Cytoplasm	Glycolysis	1.41	.21	−1.29	.3
44	Q9BTY2	Plasma alpha-L-fucosidase	5.58	54374	4	4/7	58/56	Secreted	Glycosidase	2.15	.00051	3.51	.00056
49	P13796	Plastin-2/Lymphocyte cytosolic protein 2	5.29	70814	10	6/11	58/56	Cytoplasm	Cytoskeleton regulation	2.85	NA	4.43	.0045
68	Q9NSP6	Polymerase delta-interacting protein 3	10.00	46289	14	4/16	56/56	Nucleus	Transcription control	2.3	NA	3.24	.015
512	Q9NS40	Potassium voltage-gated channel subfamily H member 7	5.75	136226	14	15/35	58/56	Plasma membrane	Transport	−1.37	.019	1.22	.033
1421	P02545	Prelamin-A/C	6.57	74380	23	19/54	95/56	Nucleus	Nuclear assembly	−1.51	.024	−1.33	.082
503	Q8IYL2	Probable tRNA (uracil-O(2)-)-methyltransferase	6.98	85944	12	9/16	73/56	Cytoplasm	Translation control	−1.86	.021	1.19	.13
683	Q15113	Procollagen C-endopeptidase enhancer 1/PCPE-1	7.41	48797	21	8/33	93/56	Secreted	Protein degradation	1.15	.23	1.59	.00086
1048	Q06323	Proteasome activator complex subunit 1	5.78	28876	30	12/34	75/56	Proteasome	Protein degradation	1.32	.0094	1.16	.013
233	P30101	Protein disulfide-isomerase A3	5.98	57146	15	9/27	76/56	ER	Protein folding	−1.28	.21	−1.47	.052
404	A6NMY6	Putative annexin A2-like protein	6.49	38806	29	11/53	64/56	Plasma membrane	Calcium regulation	−1.71	.12	1.11	.23
303	Q16740	Putative ATP-dependent Clp protease proteolytic subunit, mitochondrial	8.26	30446	22	6/28	60/56	Mitochondrion	Protein degradation	−1.53	.017	1.05	.52
297	Q16740	Putative ATP-dependent Clp protease proteolytic subunit, mitochondrial	8.26	30446	22	6/44	59/56	Mitochondrion	Protein degradation	−1.65	.027	1.12	.27
518	Q69YJ1	Putative pleckstrin homology domain containing family M member 1P	5.93	60303	16	10/41	64/56	Cytoplasm	Signal transduction	−2.10	.0018	1.18	.079
1288	Q96NR2	Putative uncharacterized protein C20orf166-AS1	11.88	14430	48	5/27	68/56	Unknown	Unknown	−1.63	.039	−1.01	.93
319	A8MTY0	Putative zinc finger protein 724	9.29	73388	17	9/18	64/56	Nucleus	Transcription control	−1.19	.17	1.38	.0093
772	Q9UQ19	Rab GTPase-activating protein 1-like	5.18	93396	9	9/10	84/56	Golgi apparatus	Vesicle transport	1.08	.81	1.32	.0067
571	Q8WUD1	Ras-related protein Rab-2B	7.68	24427	29	5/13	66/56	Golgi apparatus	Vesicle transport	−1.45	.028	−1.01	.98
1725	P10301	Ras-related protein R-Ras	6.43	23637	24	5/28	65/56	Plasma membrane	Signal transduction	2.66	6.60E-05	1.49	.0083
574	Q15293	Reticulocalbin-1	4.86	38866	23	8/25	76/56	ER	Ca regulation	−1.53	.0059	−1.4	.017
58	P48443	Retinoic acid receptor RXR-gamm	7.55	51580	7	4/8	57/56	Nucleus	Transcription control	2.06	.002	2.78	.0019
933	P48443	Retinoic acid receptor RXR-gamma	7.55	51580	8	5/10	69/56	Nucleus	Transcription control	1.14	.31	1.35	.05
1177	Q52LW3	Rho GTPase-activating protein 29	6.32	143514	6	7/11	87/56	Plasma membrane	Signal transduction	1.99	NA	1.56	.0044
1216	Q13464	Rho-associated protein kinase 1	5.66	159102	12	15/42	56/56	Plasma membrane	Signal transduction	1.26	.061	1.58	.013
952	P51812	Ribosomal protein S6 kinase alpha-3/S6K-alpha-3	6.41	84025	8	6/15	69/56	Cytoplasm	Translation control	−1.65	.018	−2.00	.012
394	P30153	Serine/threonine-protein phosphatase 2A 65 kDa regulatory subunit A alpha isoform	5.00	66079	15	10/21	104/56	Cytoplasm	Signal transduction	−1.70	.064	−1.10	.38
949	P36952	Serpin B5	5.72	42530	69	22/48	227/56	Secreted	Protease inhibitors	−1.58	.0047	−1.34	.0055
966	O15020	Spectrin beta chain	5.79	272526	3	7/12	61/56	Cytoplasm	Cytoskeleton	−1.36	.035	−1.1	.43
422	Q14683	Structural maintenance of chromosomes protein 1A/ SMC-1A	7.51	143771	9	11/32	71/56	Nucleus	Mitosis	−2.16	.00063	1.06	.52
1415	Q14683	Structural maintenance of chromosomes protein 1A/ SMC-1A	7.51	143771	7	9/15	65/56	Nucleus	Mitosis	−1.60	.062	1.04	.8
1684	O00560	Syntenin-1	7.05	32595	16	3/6	58/56	Plasma membrane	Cytoskeleton	2.26	.015	2.02	.012

Table 1 (*continued*)

No.	Swiss-prot No.	Protein name	pI	MW	Coverage (%)	No. Match. Peptides	Score	Subcellular location	Functional ontology	Ratio (25mM/ 5.5mM)	*P*-value	Ratio (100mM/ 5.5mM)	*P*-value
460	P48643	T-complex protein 1 subunit epsilon/TCP-1-epsilon	5.45	60089	37	33/51	231/56	Cytoplasm	Protein folding	−1.58	.0063	−1.20	.12
430	Q8NFZ5	TNFAIP3-interacting protein 2/Abin 2	6.03	49250	37	16/76	63/56	Cytoplasm	Transcription regulation	−2.07	.0047	1.17	.14
436	Q8NFZ5	TNFAIP3-interacting protein 2/Abin 2	6.03	49250	20	7/24	59/56	Cytoplasm	Transcription regulation	−2.24	.00068	1.07	.16
407	Q8NFZ5	TNFAIP3-interacting protein 2/Abin 2	6.03	49240	37	15/56	73/56	Cytoplasm	Transcription regulation	−1.85	.0028	1.19	.045
1103	P37837	Transaldolase	6.36	37688	25	9/37	90/56	Cytoplasm	Pentosephosphate pathway	−1.10	.39	−1.58	.014
1611	P13693	Translationally-controlled tumor protein/TCTP	4.84	19697	45	8/32	86/56	Cytoplasm	Calcium regulation	−1.13	.033	−1.52	.00051
1110	B4DJY2	Transmembrane protein 233	4.93	12237	30	3/11	56/56	Plasma membrane	Unknown	-1.4	.18	1.2	.43
1219	P60174	Triosephosphate isomerase	6.45	26938	41	6/22	113/56	Cytoplasm	Glycolysis	1.23	.047	−1.21	.21
1276	P06753	Tropomyosin alpha-3 chain	4.68	32856	20	10/40	73/56	Cytoplasm	Cytoskeleton regulation	1.50	.027	−1.15	.19
271	P23381	Tryptophanyl-tRNA synthetase	5.83	53747	9	5/10	72/56	Cytoplasm	Translation control	−1.46	.085	−1.41	.005
587	Q9BQE3	Tubulin alpha-1C chain	4.96	50548	30	12/36	102/56	Cytoplasm	Cytoskeleton	−1.14	.36	1.35	.047
1991	O00220	Tumor necrosis factor receptor superfamily member 10A	6.64	51254	7	4/8	57/56	Plasma membrane	Growth inhibition	1.54	.019	2.18	.00017
1867	Q15819	Ubiquitin-conjugating enzyme E2 variant 2	7.79	16409	40	8/25	73/56	Cytoplasm	Protein degradation	1.50	.0064	1.12	.21
317	Q8N3R3	Uncharacterized protein C3orf23	8.90	58458	10	9/23	58/56	Unknown	Unknown	−1.32	.057	1.28	.013
433	Q8N4H0	Uncharacterized protein C9orf68	9.22	45315	17	6/15	60/56	Unknown	Unknown	−1.45	.028	−1.32	.05
848	Q8N850	Vimentin	5.06	53677	26	11/25	101/56	Cytoplasm	Cytoskeleton	2.62	.00089	2.13	.0011
301	Q9H4T2	Zinc finger and SCAN domain containing protein 16	8.36	41451	28	11/49	70/56	Nucleus	Transcription control	−1.49	.027	1.19	.038
308	Q9H4T2	Zinc finger and SCAN domain containing protein 16	8.36	41451	28	11/54	65/56	Nucleus	Transcription control	−1.62	.04	1.08	.42
299	Q9H4T2	Zinc finger and SCAN domain containing protein 16	8.36	41451	28	10/31	67/56	Nucleus Transcription control		−1.65	.00004	1.13	.059
1088	Q8IZC7	Zinc finger protein 101	9.67	51903	26	10/32	75/56	Nucleus	Transcription control	1.38	.036	−1.14	.44
1216	Q2VY69	Zinc finger protein 284	8.77	71198	18	9/31	64/56	Nucleus	Transcription control	1.26	.061	1.58	.013
1027	Q6NSZ9	Zinc finger protein 498	7.82	62576	13	6/12	66/56	Nucleus	Transcription control	1.29	.026	−1.27	.32
1029	Q6NSZ9	Zinc finger protein 498	7.82	62576	13	8/24	58/56	Nucleus	Transcription control	1.81	.00036	1.13	.016
353	Q96JF6	Zinc finger protein 594	9.01	96698	15	13/50	74/56	Nucleus	Transcription control	−1.55	.0012	1.19	.023
1662	Q9P2J8	Zinc finger protein 624	9.13	102544	10	9/21	66/56	Nucleus	Transcription control	1.47	.22	−1.48	.38
1840	Q96BR6	Zinc finger protein 669	9.06	54273	20	9/33	66/56	Nucleus	Transcription control	2.10	.0014	1.17	.14
486	Q96BR6	Zinc finger protein 669	9.06	54273	20	9/34	65/56	Nucleus	Transcription control	−2.00	.00039	1.13	.066
297	P16415	Zinc finger protein 823	9.04	72790	14	10/33	58/56	Nucleus	Transcription control	−1.65	.027	1.12	.27
303	P16415	Zinc finger protein 823	9.04	72790	13	10/33	56/56	Nucleus	Transcription control	−1.53	.017	1.05	.52
309	P16415	Zinc finger protein 823	9.04	72790	13	10/33	56/56	Nucleus	Transcription control	−1.71	9.60E-05	1.16	.049

Average ratio of differential expression ($P<.05$) between Chang liver cells maintained in 5.5 mM, 25 mM and 100 mM glucose concentrations calculated from triplicate gels.

proteomic analysis. The results indicated that levels of 46 kDa AKAP8L, 26 kDa galectin-3, 45 kDa phosphoglycerate kinase 1, 33 kDa syntenin-1, 36 kDa aldose reductase, 24 kDa glutathione S-transferase P, 52 kDa retinoic acid receptor RXR-gamma, 27 kDa triosephosphate isomerase, and 54 kDa vimentin levels were significantly elevated in the plasma of diabetic patients compared to plasma from healthy donors. These proteins might, therefore, be potential candidates for the diagnosis of diabetic liver disease. Levels of 72 kDa GRP-78, 26 kDa CD63 and 49 kDa Abin 2 were markedly lower in the plasma of patients with diabetic liver disease compared to plasma from healthy controls. These findings were consistent with data from 2D-DIGE and MALDI-TOF MS and further suggested that the identified proteins could potentially be used as indicators of diabetic liver disease (Fig. 6).

With the basis of a Swiss-Prot search and KEGG pathway analysis, numerous potential biological functions of the identified proteins across Chang liver cells maintained in mannitol-balanced 5.5 mM and 25 mM glucose were determined. This information could be useful for studying

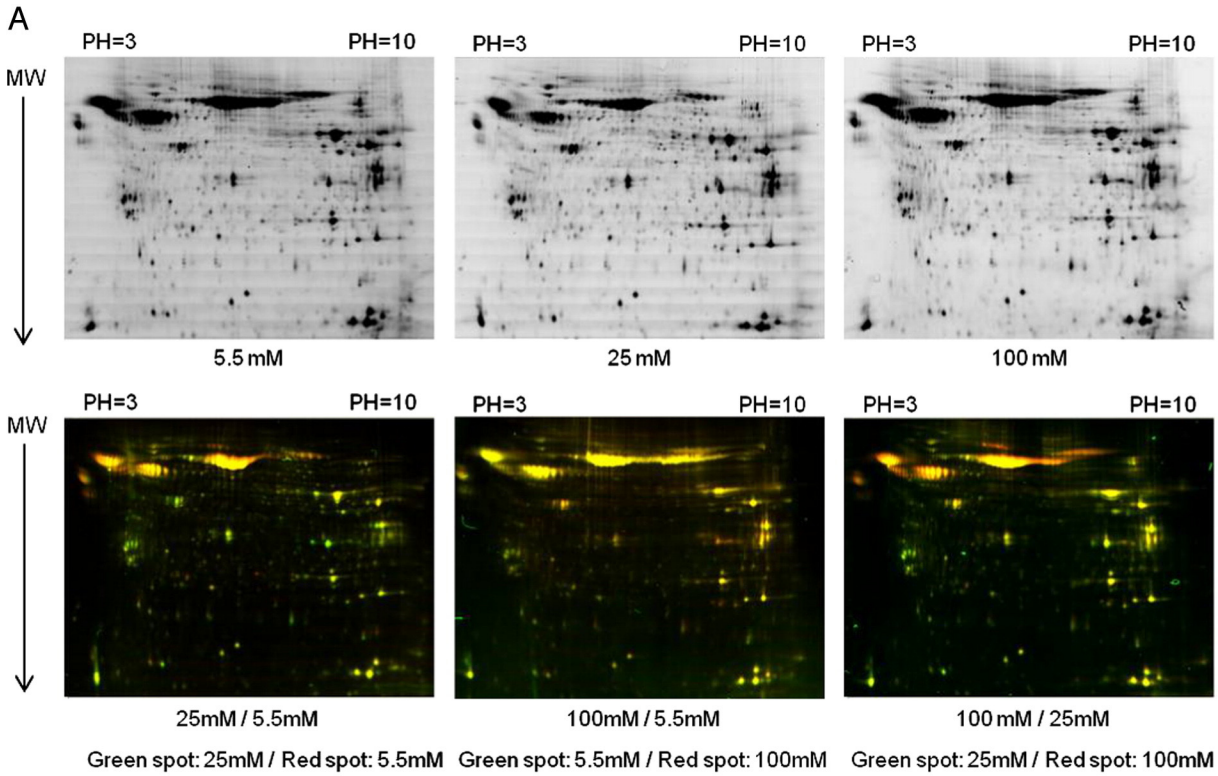

Fig. 2. 2D-DIGE analysis of high glucose-dependent differentially expressed proteins in Chang liver cells. Chang liver cells maintained in 5.5 mM, 25 mM and 100 mM glucose were lysed and arranged for a triplicate 2D-DIGE experiment. Protein samples (150 μg each) were labeled with Cy-dyes and separated using 24 cm, pH 3–10 non-linear IPG strips. 2D-DIGE images of Chang liver incubated in 5.5 mM, 25 mM and 100 mM glucose at appropriate excitation and emission wavelengths were pseudo-colored and overlaid with ImageQuant Tool (GE Healthcare). The differentially expressed identified protein features are annotated with spot numbers.

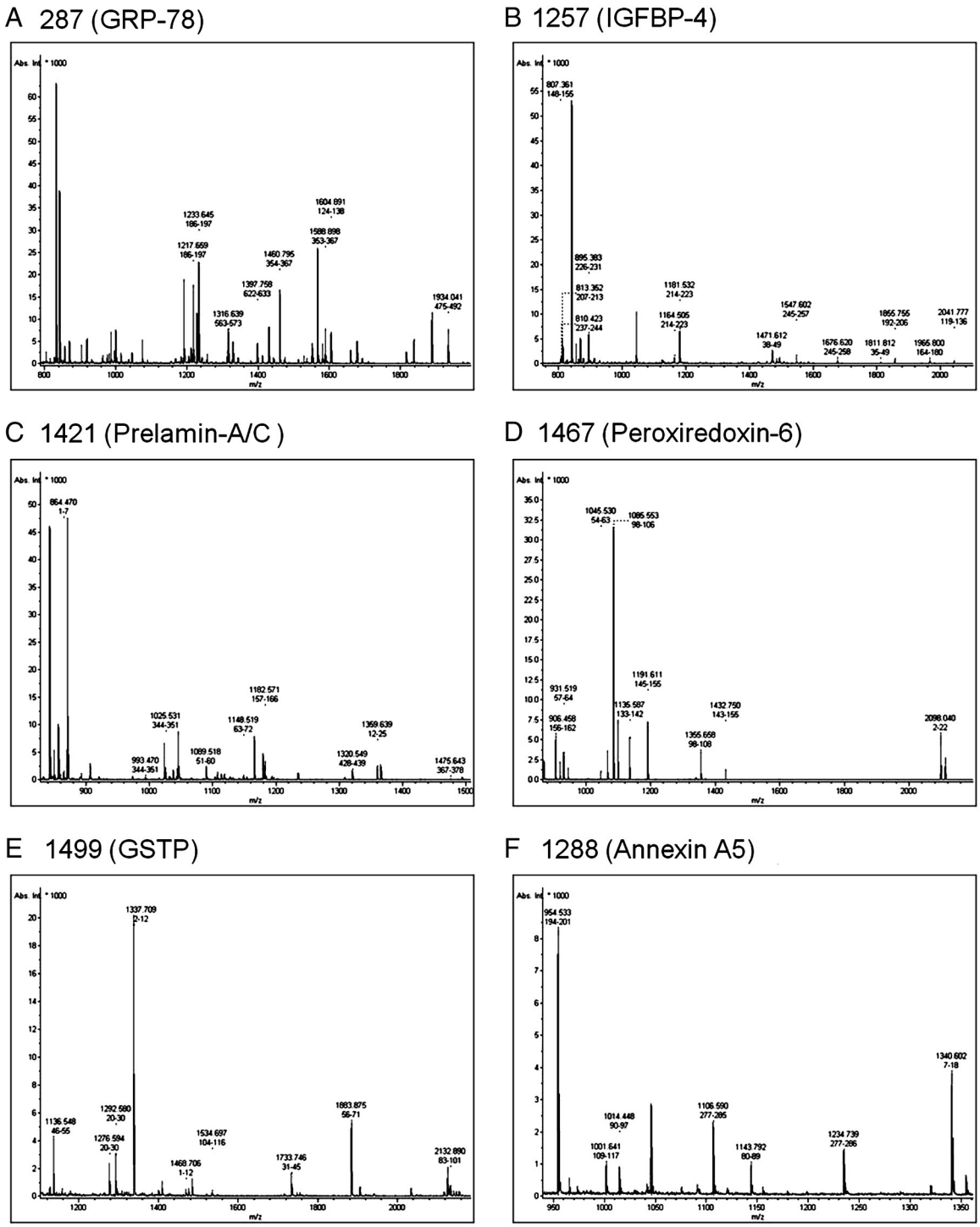

Fig. 3. Peptide mass fingerprinting of differentially expressed proteins [(A) GRP-78 (B) IGFBP-4 (C) Prelamin A/C (D) Peroxiredoxin-6 (E) GST-pi (F) Annexin 5]. Mass spectra were acquired on an Autoflex TOF/TOF mass spectrometer (Bruker Daltonics). Peptides contribute to protein identifications were marked with *m/z* values and sequence locations on proteins which were searched against the Swiss-Prot/TrEMBL database (2011_08, 531473 sequence entries) using Mascot software v2.3.02 (Matrix Science, London, UK).

the mechanisms of high glucose level-induced liver disease. Fig. 7 compares the expression profiles of the identified differentially expressed proteins in these 2 cell conditions. We discovered that proteins known to regulate calcium signaling and translation control were down-regulated in 25 mM glucose-cultured Chang liver cells (Fig. 7A and H). In contrast, the expression of proteins linked to cytoskeleton regulation, glycolysis, mitosis, protein degradation, protein folding, redox regulation and vesicle transport were up-regulated in the 25 mM glucose-cultured Chang liver cells compared to the levels in 5.5 mM glucose-cultured Chang liver cells (Figs. 7B, C, D, E, F, G, and I).

3.3. Redox proteomic analysis of high glucose-induced cysteine modifications in Chang liver cell proteins

High glucose concentrations reportedly induce ROS, which can damage liver cells through glycoxidation and cause diabetic liver

disease. Although cellular antioxidant reactions can balance low ROS concentrations, the accumulation of ROS induces modifications in biomolecules such as proteins, lipids and DNA. The reduced thiol group of cysteine residues is a potent nucleophilic agent that undergoes numerous oxidative modifications, leading to loss of protein function (see Introduction). To optimize conditions for the monitoring of oxidative stress-induced protein modifications, we used DCF fluorescence to detect high glucose level-induced ROS production. The results showed that high glucose concentrations increased ROS production in Chang liver cells (Fig. 8). We then applied the recently developed redox 2D-DIGE strategy using ICy dyes to evaluate alterations in protein thiol reactivity induced by high glucose concentrations. We compared Chang liver cells cultured in high glucose concentrations (25 mM) with Chang liver cells cultured in 5.5 mM glucose. These cells were lysed in the presence of ICy5, in triplicate. Individual ICy5-labeled samples were then run on 2-DE against an equal load of ICy3-labeled standard pool samples, consisting of an equal mixture of 3 sample types to aid in spot matching, to improve the accuracy of quantification (Fig. 9). The ICy5-labeled samples were subsequently labeled with lysine labeling Cy2 dye as an internal protein level control, which was used to normalize the corresponding ICy5/ICy3 signals (Table 2). We detected 2125 protein features, of which 81 displayed statistically significant changes in labeling in response to high glucose concentrations. A comparison of our saturated cysteine-labeling 2D-DIGE images with the images obtained using the minimal lysine-labeling strategy

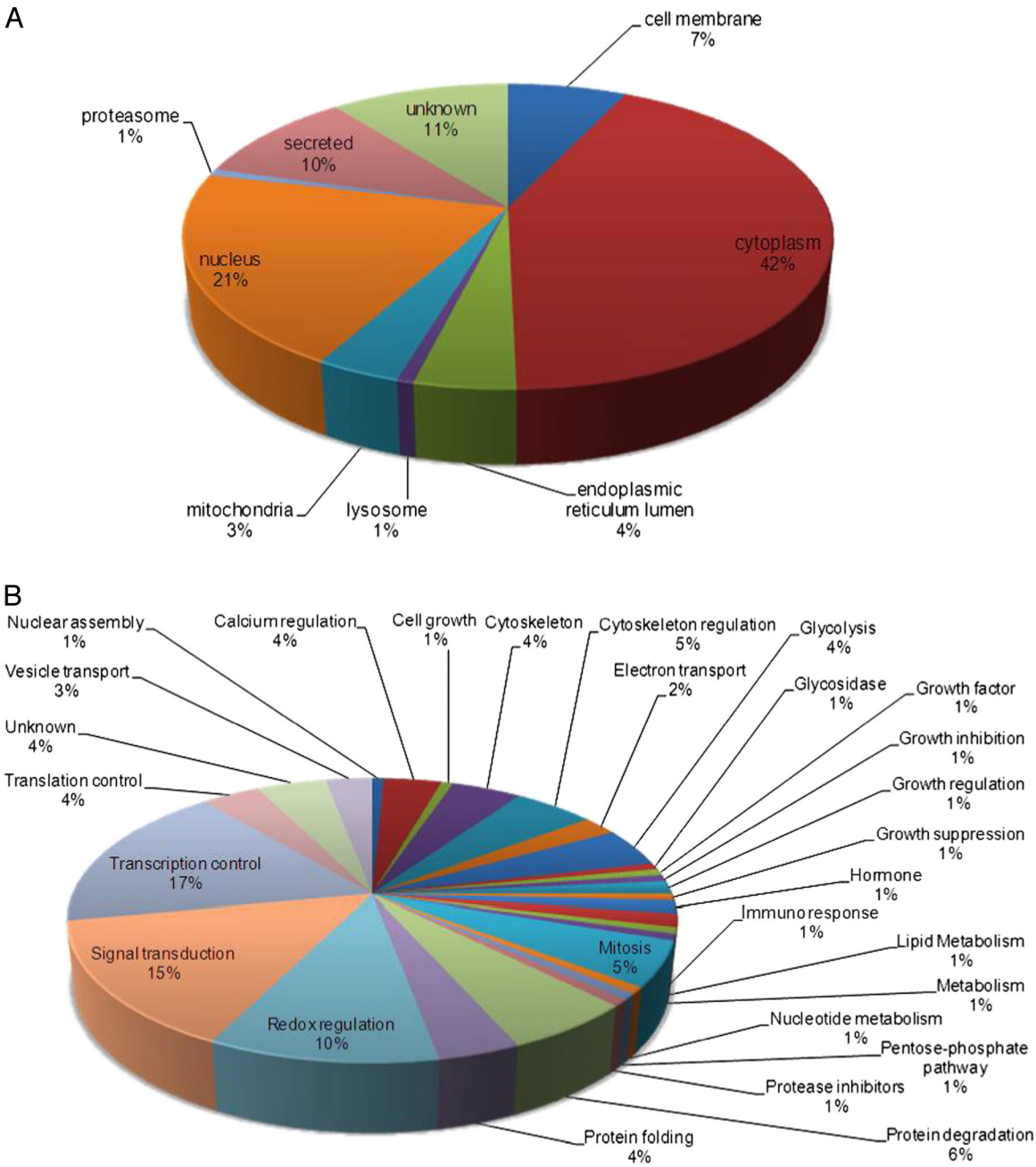

Fig. 4. Percentage of differentially expressed proteins identified by 2D-DIGE / MALDI-TOF MS for Chang liver cells incubated in 5.5 mM, 25 mM and 100 mM glucose according to their sub-cellular locations (A) and biological functions (B). The classification of the biological functions and sub-cellular locations of these identified proteins are based on a Swiss-Prot search and KEGG pathway analysis.

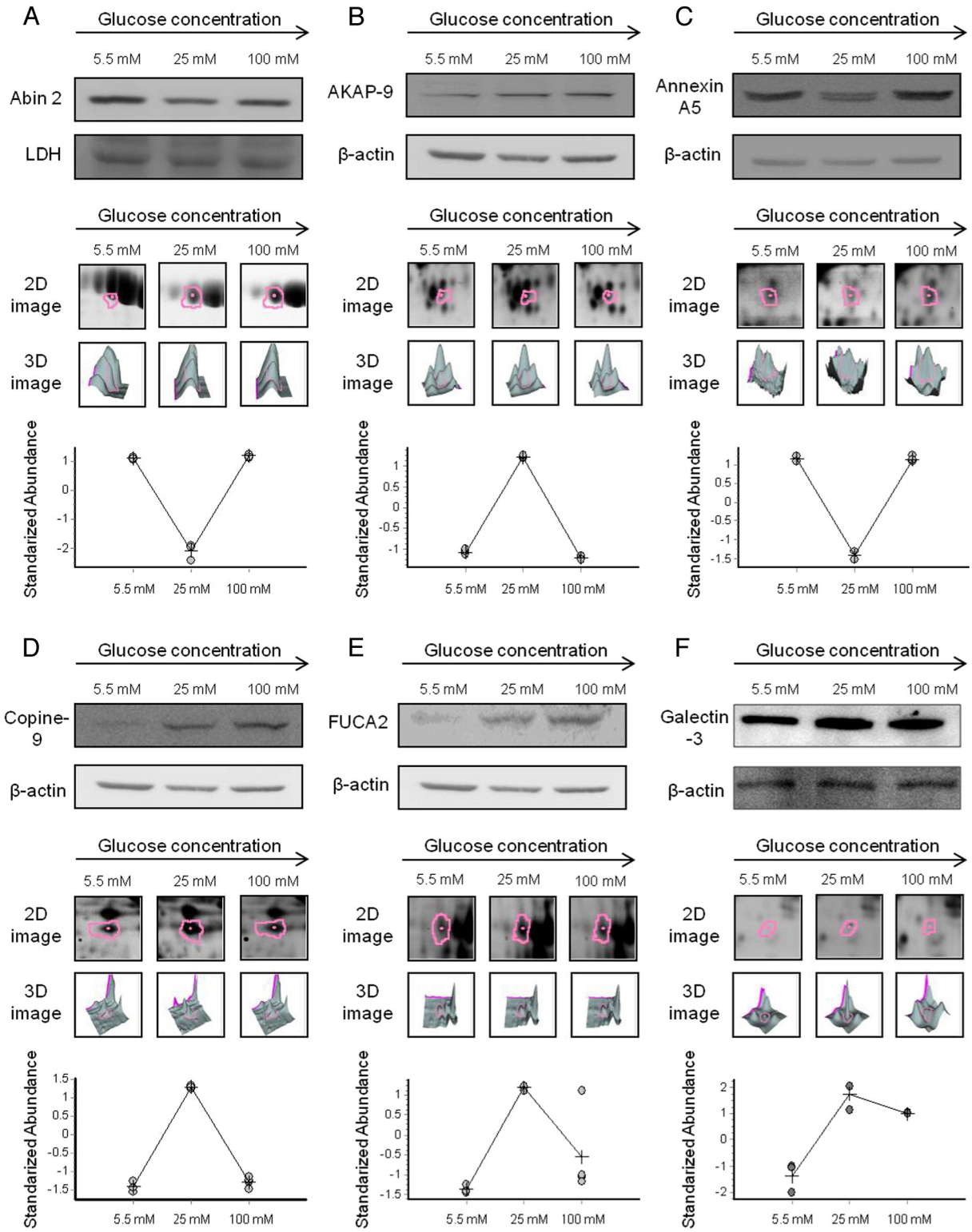

Fig. 5. Representative immunoblotting analyses and 2D-DIGE images for selected differentially expressed proteins [(A) Abin 2 (B) AKAP-9 (C) Annexin 5 (D) Copine-9 (E) FUCA2 (F) Galectin-3 (G) GRP 78 (H) GSTP1 (I) IGFBP2 (J) IGFBP4 (K) L-plastin (L) Lamin A/C (M) MPR (N) PDI (O) PGK 1 (P) PI-TP-β (Q) Prx-6 (R) RSK2 (S) RXR-γ (T) Syntenin-1 (U) Vimentin] identified by 2D-DIGE/MALDI-TOF MS for Chang liver cells incubated in 5.5 mM, 25 mM and 100 mM glucose. The levels of identified proteins in Chang liver cells maintained in 5.5 mM, 25 mM and 100 mM glucose were confirmed by immunoblot (top panels). Beta-actin or LDH were used as loading controls in this study. The levels of these intracellular proteins were also visualized by fluorescence 2-DE images (middle top panels), three-dimensional spot images (middle bottom panels) and protein abundance maps (bottom panels).

revealed that precipitation increased significantly in proteins in the >70 kDa molecular weight range. The presence of ICy dye-modified cysteines in higher molecular weight proteins might have caused the observed increases in precipitation. We then performed post-staining with CCB and matched the stains with fluorescence images, to select 82 gel features. We identified 29 of these features as unique gene

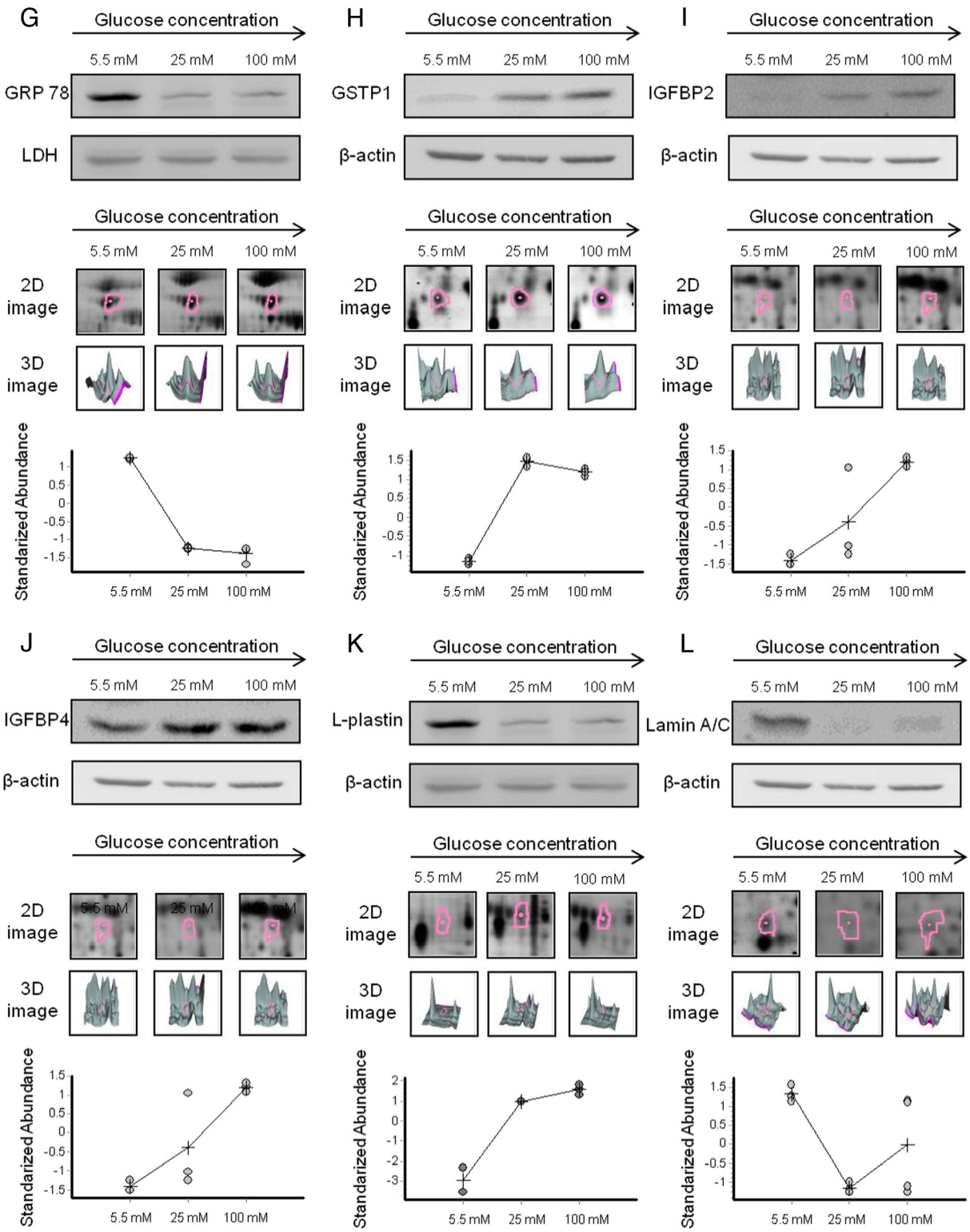

Fig. 5 (*continued*).

products using MALDI-TOF peptide mass fingerprinting (Table 2). All of the identified proteins contained at least one cysteine (retrieved from the Swiss-Prot database). Because the ICy dyes target reduced cysteinyl thiols, these results suggested that the high glucose concentration modified the oxidative status of some of the thiol groups. We classified the identified proteins according to their subcellular locations and biological functions: 53% of the proteins were cytosolic, 13% were endoplasmic reticulum proteins, 13% were nuclear proteins, 9% were mitochondrial proteins, 6% were secreted proteins and 6% were located in plasma membranes. The identified proteins were predominantly involved in metabolism (25%), transport (18%) and cell apoptosis (12%) (Fig. 10).

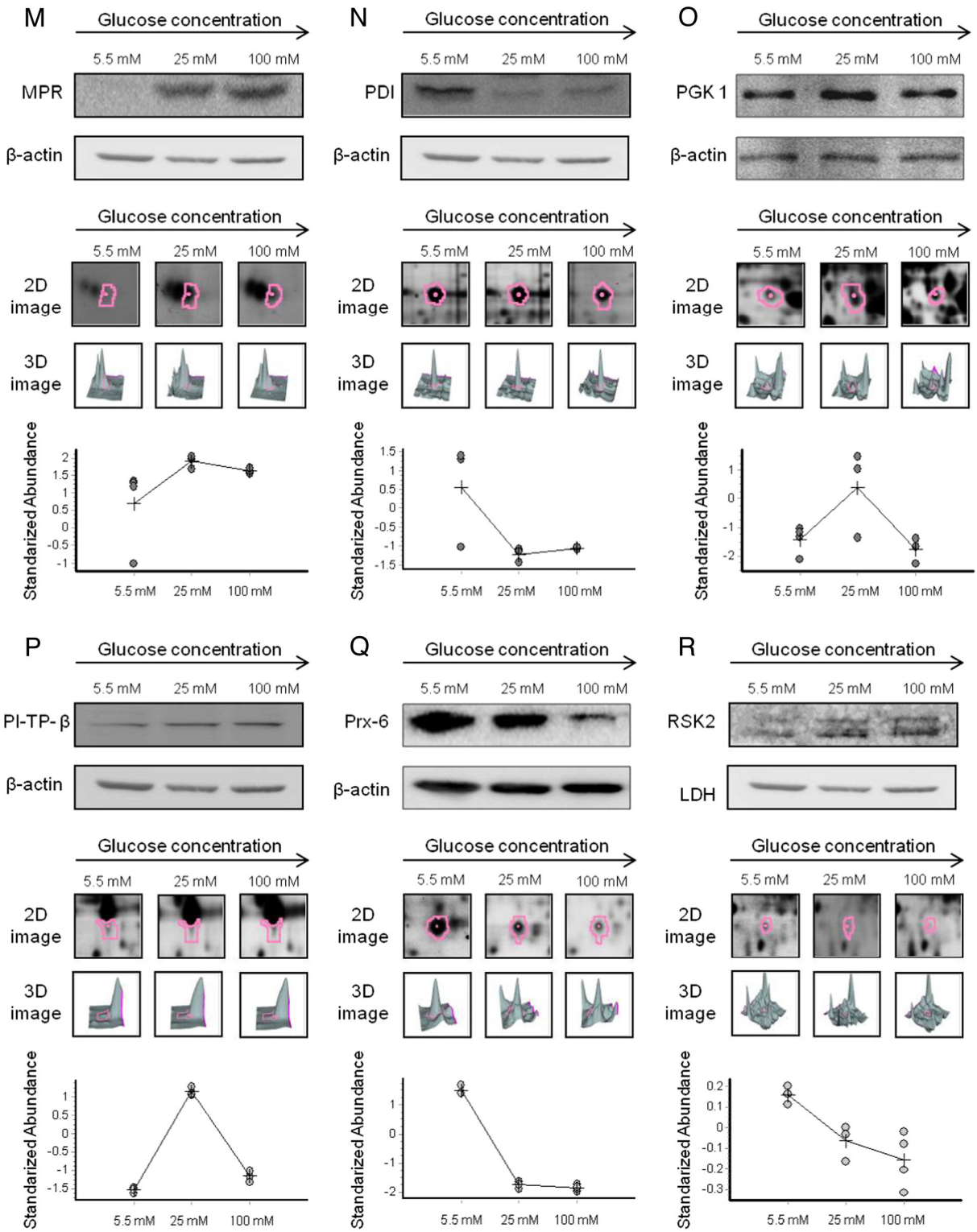

Fig. 5 (*continued*).

4. Discussion

In this study, we evaluated high glucose level-induced changes in protein expression and thiol reactivity in Chang liver cells using lysine- and cysteine-labeling 2D-DIGE. One hundred forty-one proteins showed differential expression in Chang liver cells cultured in high glucose concentrations, compared with control Chang liver cells. More than one third of the proteins exhibited glucose concentration-dependent changes in expression in Chang liver cells cultured in 5.5 mM, 25 mM, and 100 mM glucose. However, almost two thirds of the identified proteins, including annexin A5, failed to display glucose concentration-dependent changes in expression in 100 mM glucose. This suggested that very high glucose concentrations might activate mechanisms

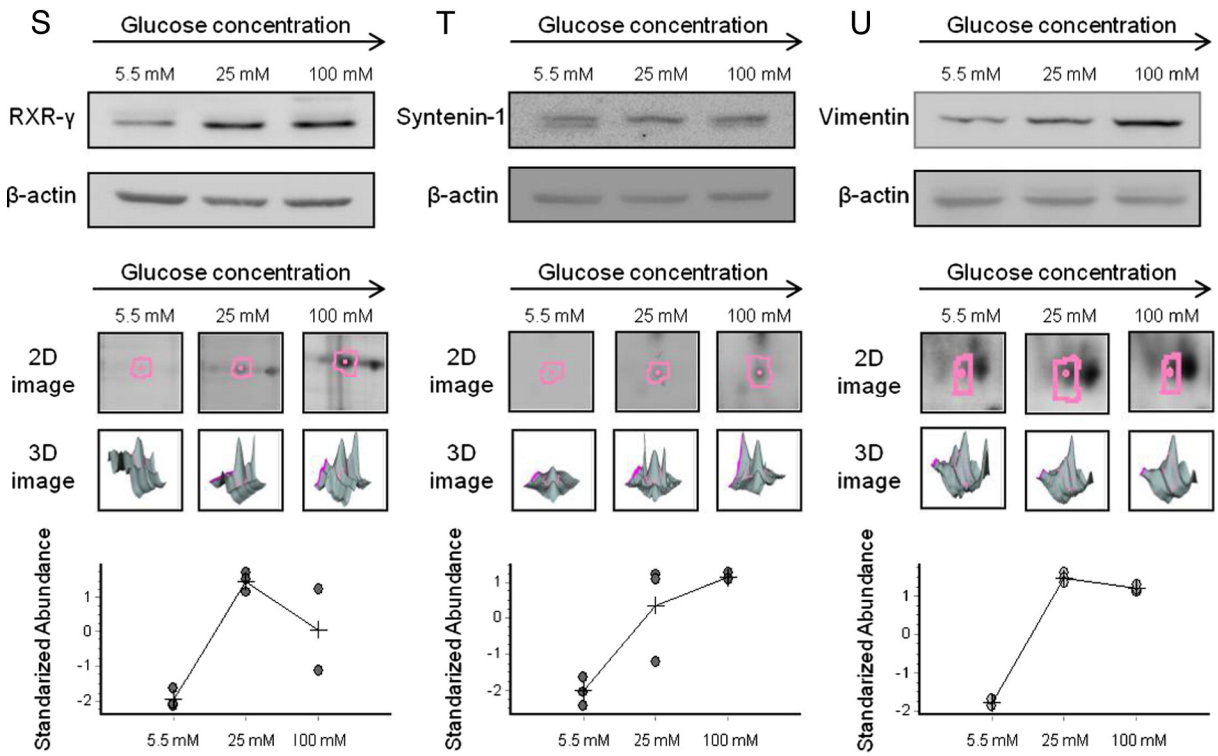

Fig. 5 (*continued*).

yet to be identified, to reverse high glucose-induced changes in protein expression.

Previous studies have shown that high glucose concentrations induce the production of superoxide radicals through the auto-oxidation of glucose in vitro [19,20]. Studies have also highlighted increases in protein-oxidation products in the blood of diabetic patients. The most extensively investigated markers of protein oxidation are protein carbonyl groups, which result in the formation of oxidized side chains on proline, lysine, arginine and threonine residues [24–26]. Cysteine is also highly susceptible to ROS-induced oxidation [24]. Our redox-proteomic results indicated that long-term incubation of cultured hepatocytes in high concentrations of glucose led to the oxidation of thiol groups on cysteine residues. Further evidence indicated that these cellular proteins were the intracellular targets of gluco-oxidation. By analyzing changes in thiol reactivity in response to high glucose levels, we identified 29 proteins that showed redox changes in the cysteine residues of specific proteins. Our findings suggest that high glucose level-induced oxidative stress disturbed the normal redox balance in Chang liver cells, leading to the redox modulation of specific proteins. The ICy labeling results supported the hypothesis that high glucose concentrations induce the formation of free thiols in certain proteins by breaking disulfide bonds, which increases ICy dye labeling. In addition, high glucose concentrations that induced ROS or protein-derived peroxides might then directly oxidize thiol groups to form the sulfenic, sulfinic or sulfonic acid forms of cysteine, leading to decreased ICy dye labeling. These thiol modifications have been reported to disturb normal protein function [38]. Our results suggest that high glucose concentrations induce changes in protein expression and redox regulation that modify cell physiology and might contribute to the development of diabetic liver diseases.

We observed that proteins involved in redox regulation (aldose reductase, biliverdin reductase A, glutathione S-transferase, pericentrin, peroxiredoxin-1, peroxiredoxin-6 and trimethyllysine dioxygenase) and protein folding (GRP-78, HSP-60, HSP-70, HSP-beta 1, cyclophilin A) display altered expression or altered thiol reactivity in high glucose concentrations. Heat-shock proteins are molecular chaperones that protect cells from harmful conditions by reducing the concentrations of denatured or unfolded proteins. The accumulation of damaged and misfolded proteins following exposure to toxic stimuli is a major cause of cell death [39]. Previous reports indicated that physiological and environmental stresses, including high glucose concentration-induced oxidative stress, up-regulate the expression of peptidyl-prolyl cis-trans isomerase A and peroxiredoxin-1. Ramachandran et al. [40] reported that peptidyl-prolyl cis-trans isomerase A is secreted by monocytes in response to high glucose-level treatment, and the protein is a potential secretory marker of inflammation in type 2 diabetes. In addition, peroxiredoxin-1 is up-regulated in the early phase of liver ischemia reperfusion injury in response to high glucose-induced oxidative stress [41]. Our results indicate that high glucose concentrations up-regulate the expression of heat-shock and redox regulating proteins in hepatocytes and influence their thiol reactivity. Further analyses using redox proteomic strategies confirmed the involvement of the identified proteins in protein folding and redox regulation in Chang liver cells. HSP-70, HSP-beta 1 and peroxiredoxin-1 all showed increased labeling in high glucose concentrations, suggesting that high glucose concentrations directly modulate the functions of these proteins by generating new free thiol groups. In contrast, HSP-60, cyclophilin A and trimethyllysine dioxygenase all exhibited decreased labeling in high glucose concentrations, implying that high glucose concentrations directly regulate the biological functions of the identified proteins via oxidation of the free thiol group on cysteine.

The up-regulation of heat-shock proteins also suggests the increased expression of unfolded proteins in the endoplasmic reticulum (ER), which correlates with ER stress [42]. Several previous reports have identified ER stress in diabetes, observing increased levels of ER stress markers such as BiP, CHOP and GRP94 in a diabetic

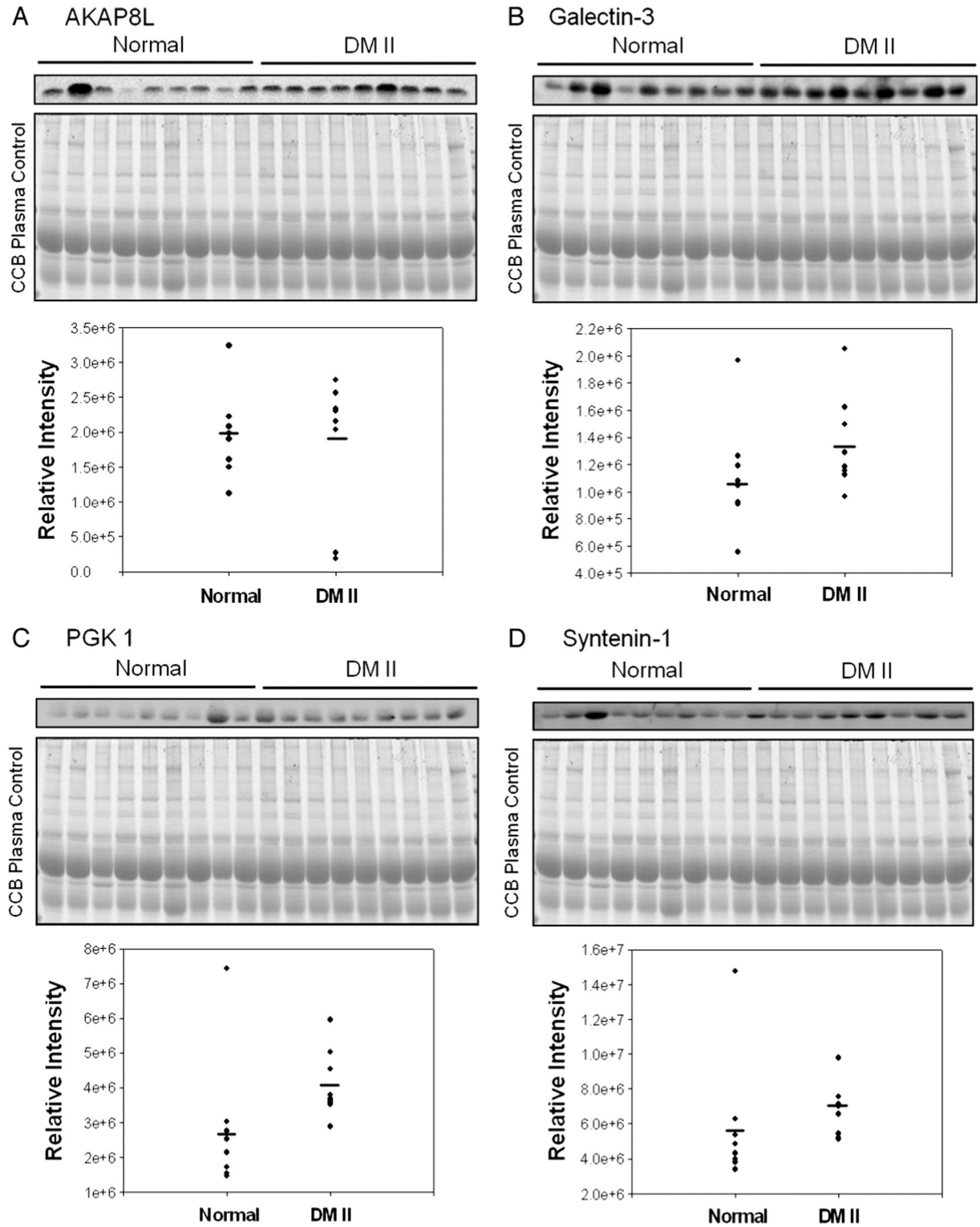

Fig. 6. Representative immunoblotting and ELISA analysis of AKAP8L, Galectin-3, PGK 1, Syntenin-1, Abin 2, Aldose reductase, CD63, GRP-78, GST-pi, RXR-gamma, TPI and Vimentin in plasma from Type 2 diabetic patients with liver disease and healthy donors. Plasma samples from 10 type 2 diabetic patients and 10 healthy donors were run in a pool. 20 μg of plasma samples were loaded and resolved by SDS-PAGE followed by either immumoblotting with (A) AKAP8L, (B) Galectin-3, (C) PGK 1 and (D) Syntenin-1 antibodies or staining with colloidal coomassie Blue G-250 as a loading control. (E–L) 50 μg of plasma samples were coated onto each well of 96-well plate for ELISA analysis against Abin 2, aldose reductase, CD63, GRP-78, GST-pi, RXR-gamma, TPI, vimentin and the absorbance was measured at 450nm using a Stat Fax 2100 microtiterplate reader. Paired Student's *t* test has been used for the statistical analysis of the experimental results. The statistic comparisons used in this study were performed with two group paired Student's *t* test.

mouse model [43] and in pancreatic beta cells of type 2 diabetic patients [44]. The ER plays an important role in regulating intracellular Ca^{2+} concentrations. Endoplasmic reticulum stress might contribute to Ca^{2+} release from the ER and stimulate mitochondrial disruption, which then suppresses cell survival [45]. We observed that high glucose concentrations decreased heat shock in 70 kDa protein 5

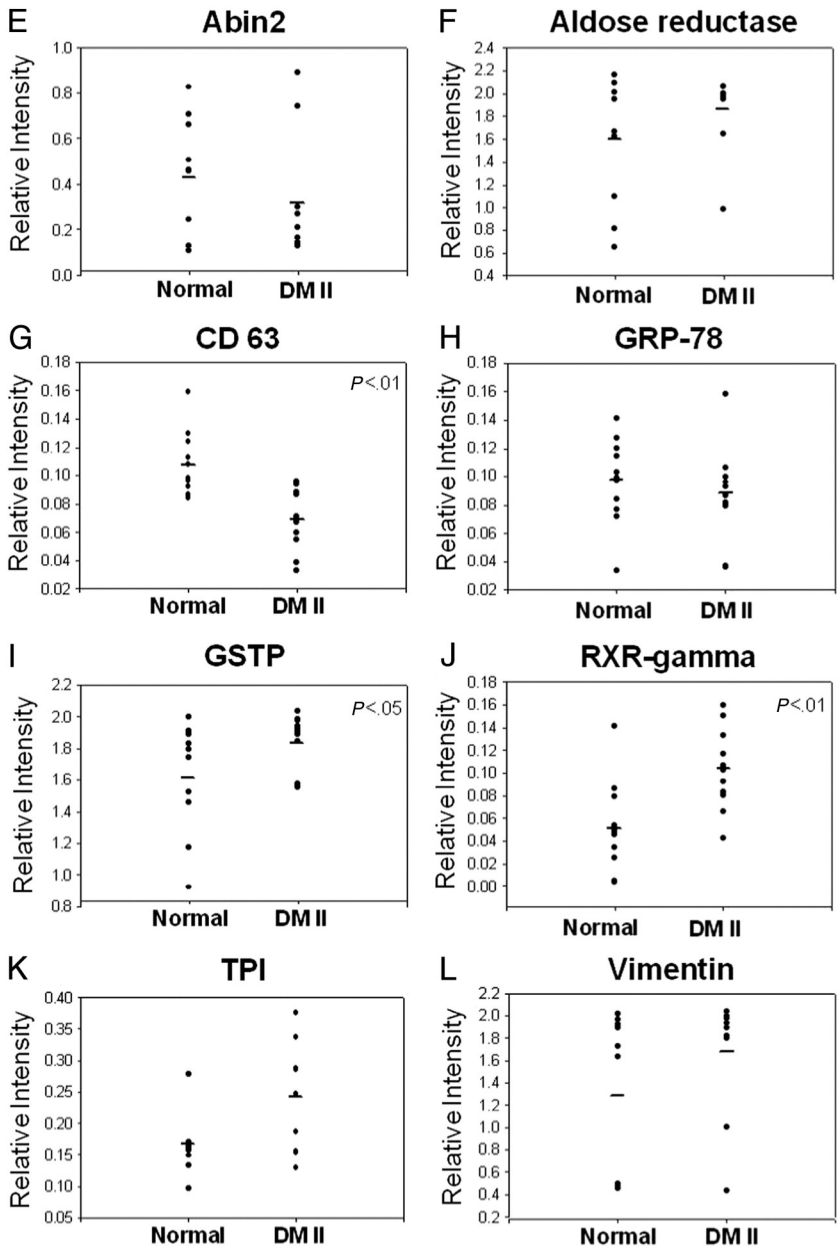

Fig. 6 (*continued*).

(GRP78), an ER chaperone protein responsible for maintaining the accurate folding of ER proteins, leading to ER stress. This mechanism might explain alterations in the expression and activation of Ca^{2+}-dependent proteins (such as annexin A4, annexin A5, reticulocalbin-1 and translationally-controlled tumor protein) in Chang liver cells treated with high glucose concentrations, compared with control cells. Protein kinase C (PKC) is a member of the family of protein kinases responsible for controlling the phosphorylation and activation of downstream target proteins. Numerous studies have reported that Ca^{2+} and diacylglycerol signaling activate PKC [46,47]. To examine the hypothesis that increased Ca^{2+}, derived from high glucose concentration-induced phosphorylation of downstream targets, stimulates PKC, we performed an immunoblot analysis of phospho-PKC substrates. We found that multiple PKC substrates showed increased phosphorylation in Chang liver cells cultured in 25 mM and 100 mM glucose, compared with cells cultured in 5.5 mM glucose (Fig. 11).

The retinoid X receptor (RXR) belongs to a family of nuclear receptors which are stimulated by retinoic acid, and play essential roles as ligand-driven transcription factors in fundamental bioprocesses such as glucose homeostasis. The RXR can form functional heterodimers with numerous nuclear receptors, including the vitamin

Fig. 7. Expression profiles for proteins potentially contributing to (A) calcium regulation, (B) cytoskeleton regulation, (C) glycolysis, (D) mitosis, (E) protein degradation, (F) protein folding, (G) redox regulation, (H) translation control, and (I) vesicle transport in comparing Chang liver cells maintained in mannitol-balanced 5.5 mM and 25 mM glucose. Red bars and green bars represent fold up-regulation and down-regulation in protein expression in cell maintained in mannitol-balanced 25 mM glucose versus cell maintained in mannitol-balanced 5.5 mM glucose, respectively. The vertical axis indicates the identified proteins; the horizontal axis indicates the fold change in protein expression. Additional details for each protein can be found in Table 1.

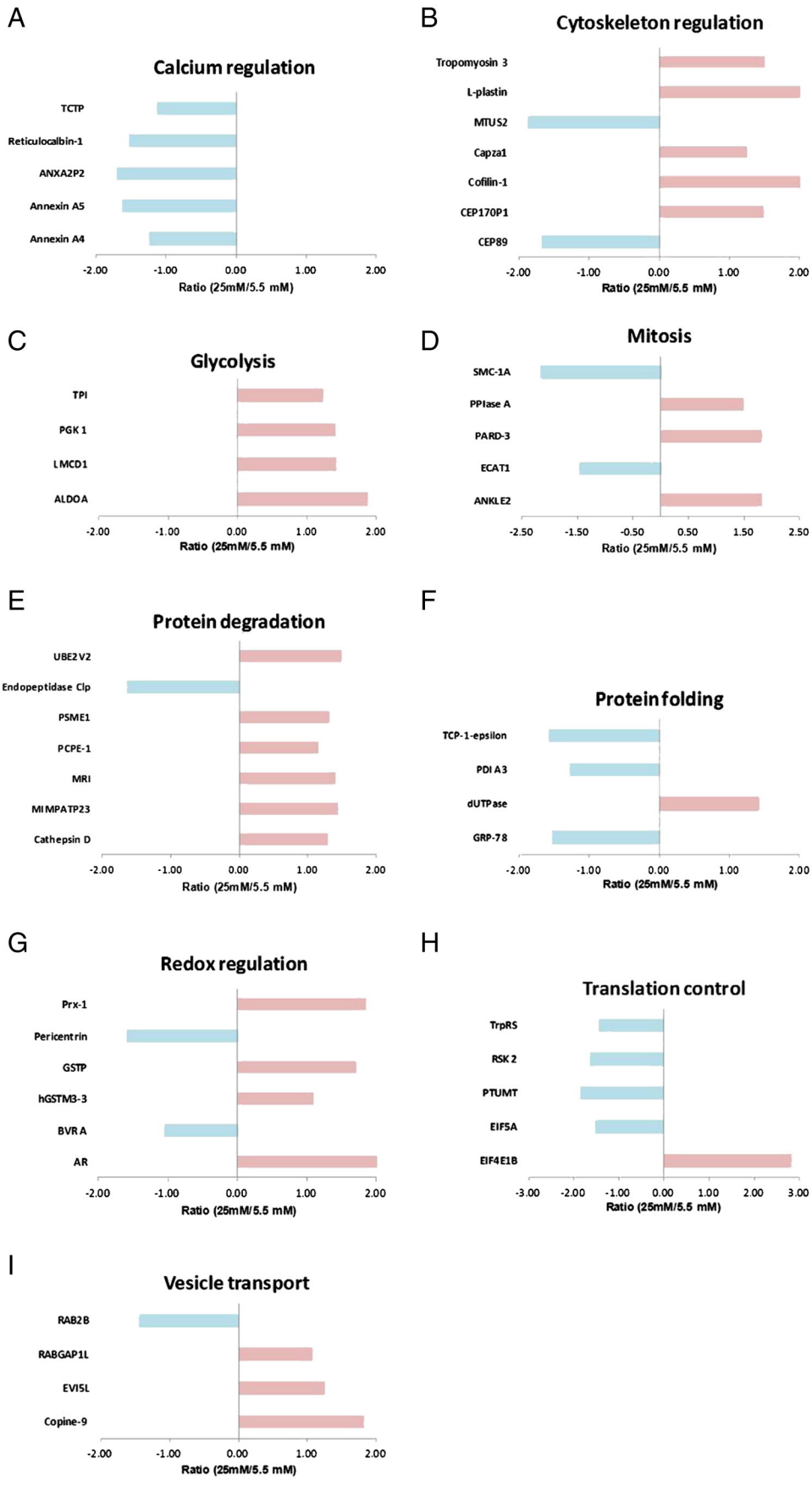
A
Calcium regulation
TCTP
Reticulocalbin-1
ANXA2P2
Annexin A5
Annexin A4
-2.00 -1.00 0.00 1.00 2.00
Ratio (25mM/5.5 mM)
B
Cytoskeleton regulation
Tropomyosin 3
L-plastin
MTUS2
Capza1
Cofilin-1
CEP170P1
CEP89
-2.00 -1.00 0.00 1.00 2.00
Ratio (25mM/5.5 mM)
C
Glycolysis
TPI
PGK 1
LMCD1
ALDOA
-2.00 -1.00 0.00 1.00 2.00
Ratio (25mM/5.5 mM)
D
Mitosis
SMC-1A
PPIase A
PARD-3
ECAT1
ANKLE2
-2.50 -1.50 -0.50 0.50 1.50 2.50
Ratio (25mM/5.5 mM)
E
Protein degradation
UBE2V2
Endopeptidase Clp
PSME1
PCPE-1
MRI
MIMPATP23
Cathepsin D
-2.00 -1.00 0.00 1.00 2.00
Ratio (25mM/5.5 mM)
F
Protein folding
TCP-1-epsilon
PDIA3
dUTPase
GRP-78
-2.00 -1.00 0.00 1.00 2.00
Ratio (25mM/5.5 mM)
G
Redox regulation
Prx-1
Pericentrin
GSTP
hGSTM3-3
BVRA
AR
-2.00 -1.00 0.00 1.00 2.00
Ratio (25mM/5.5 mM)
H
Translation control
TrpRS
RSK 2
PTUMT
EIF5A
EIF4E1B
-3.00 -2.00 -1.00 0.00 1.00 2.00 3.00
Ratio (25mM/5.5 mM)
I
Vesicle transport
RAB2B
RABGAP1L
EVI5L
Copine-9
-2.00 -1.00 0.00 1.00 2.00
Ratio (25mM/5.5 mM)

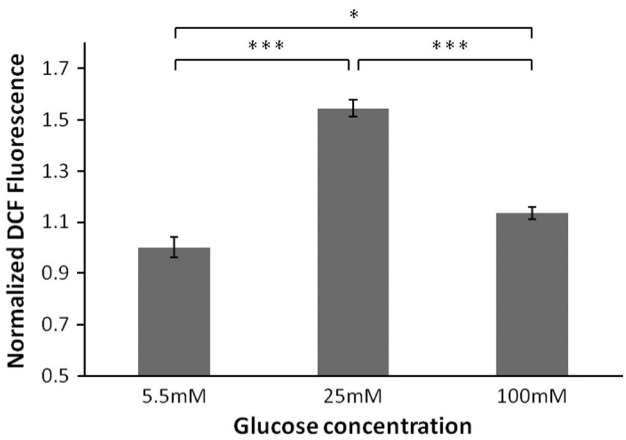

Fig. 8. Effect of high glucose on Chang liver cell ROS production. DCFH-based intracellular ROS production assays were performed where 10,000 Chang liver cells cultured in 5.5 mM, 25 mM and 100 mM glucose for at least 3 weeks were plated into 96-well plates in medium containing 10% FBS. After overnight incubation in 5.5 mM, 25 mM and 100 mM glucose, the cells were treated with 10 μM of DCFH-DA at 37°C for 20 min and the fluorescence images was recorded at excitation and emission wavelengths of 485 nm and 530 nm, respectively. Paired Student's *t* test has been used for the statistical analysis of the experimental results. ***$P \leq .001$.

D receptor and the retinoic acid receptor (RAR) [48]. Previous reports demonstrated that oxidative stress and JNK signaling act as mediators in response to high glucose concentration-induced suppression of the RAR/RXR complex in cardiomyocytes [49]. Reducing oxidative stress can bring back RAR/RXR signaling and protect cardiomyocytes from hyperglycemia [50]. Additionally, RXR prevented the reduction of the retinal pigmented epithelium cell viability, and maintained the normal function and survival of the cells by disorganizing and shortening their outer segments and reducing light responses in a mouse model [51]. Our data indicates that high glucose concentrations upregulated RXR expression in human hepatocytes, and in turn, might stimulate RAR/RXR signaling and the interactions between RXR and other nuclear receptors. Accordingly, high glucose levels promote the protective ability of RXR in liver cells, and increase the cell viability of hepatocytes against hyperglycemia.

The 4 proteins (AKAP8L, galectin-3, PGK 1 and syntenin-1) identified by immunoblotting, and the 8 proteins (Abin 2, aldose reductase, CD63, GRP-78, GST-pi, RXR-gamma, TPI and vimentin) identified by ELISA have shown differential expression in clinical plasma, suggesting these proteins are potential disease-markers for diabetic liver diseases (Fig. 6). Crucially, not all of these proteins have been reported as markers for diabetic liver diseases, further implying that they might not only be evaluated as disease-markers for the disease, but also help to clarify the detailed mechanisms in diabetic liver disease-associated regulation. Furthermore, combinations of these identified proteins have not yet been described as markers for other diseases. Accordingly, the combination of these identified proteins could be evaluated as diabetic liver disease-specific markers.

In summary, in this study we performed comprehensive proteomic analyses of liver cells cultured in various concentrations of glucose. We identified differentially expressed proteins, and developed a redox proteomic platform for the monitoring of redox-modulated proteins in Chang liver cells, following their treatment with high glucose concentrations. We identified high glucose concentration-modulated proteins that participate in several cellular responses including transcription control, signal transduction, redox regulation, cytoskeleton regulation, protein folding and gene regulation. Our study results indicate the presence of an entire network of proteins in liver cells exposed to high glucose concentrations that might play roles in the development of diabetic liver disease. A comparison of plasma specimens from patients with type 2 diabetic liver disease and those from healthy donors confirmed the changes in expression of 12 proteins (AKAP8L, galectin-3, PGK 1, syntenin-1, Abin 2, aldose reductase, CD63, GRP-78, GST-pi, RXR-gamma, TPI and vimentin) in diabetic liver disease. Our findings indicate potential markers of diabetic liver disease that are suitable for early-stage evaluation of disease prognosis. The identified proteins might also represent potential targets for treatment of hyperglycemia-induced liver disease.

Acknowledgments

This work was supported by NSC grant (NSC 101-2311-B-007-011) from National Science Council, Taiwan and Toward word-class university project and Nano- and Micro- ElectroMechanical Systems-based Frontier Research on Cancer Mechanism, Diagnosis and Treatment grant from National Tsing Hua University, Taiwan.

Declaration of competing interests.

The authors confirm that there are no conflicts of interest.

References

[1] Gillery P. Oxidative stress and protein glycation in diabetes mellitus. Ann Biol Clin (Paris) 2006;64:309–14.
[2] Yan SF, Ramasamy R, Schmidt AM. Receptor for AGE (RAGE) and its ligands-cast into leading roles in diabetes and the inflammatory response. J Mol Med (Berl) 2009;87:235–47.
[3] Boulanger E, Wautier JL, Dequiedt P, Schmidt AM. Glycation, glycoxidation and diabetes mellitus. Nephrol Ther 2006;2(Suppl. 1):S8–S16.
[4] Vlassara H. The AGE-receptor in the pathogenesis of diabetic complications. Diabetes Metab Res Rev 2001;17:436–43.
[5] Zill H, Gunther R, Erbersdobler HF, Folsch UR, Faist V. RAGE expression and AGE-induced MAP kinase activation in Caco-2 cells. Biochem Biophys Res Commun 2001;288:1108–11.
[6] Yang H, Jin X, Wai Kei LC, Yan SK. Review: oxidative stress and diabetes mellitus. Clin Chem Lab Med 2011;49:1773–82.
[7] Sauvaget D, Chauffeton V, Dugue-Pujol S, Kalopissis AD, Guillet-Deniau I, Foufelle F, et al. In vitro transcriptional induction of the human apolipoprotein A-II gene by glucose. Diabetes 2004;53:672–8.
[8] Zang M, Zuccollo A, Hou X, Nagata D, Walsh K, Herscovitz H, et al. AMP-activated protein kinase is required for the lipid-lowering effect of metformin in insulin-resistant human HepG2 cells. J Biol Chem 2004;279:47898–905.
[9] Nakajima K, Yamauchi K, Shigematsu S, Ikeo S, Komatsu M, Aizawa T, et al. Selective attenuation of metabolic branch of insulin receptor down-signaling by high glucose in a hepatoma cell line, HepG2 cells. J Biol Chem 2000;275:20880–6.
[10] Schafer FQ, Buettner GR. Redox environment of the cell as viewed through the redox state of the glutathione disulfide/glutathione couple. Free Radic Biol Med 2001;30:1191–212.
[11] Lim JC, Choi HI, Park YS, Nam HW, Woo HA, Kwon KS, et al. Irreversible oxidation of the active-site cysteine of peroxiredoxin to cysteine sulfonic acid for enhanced molecular chaperone activity. J Biol Chem 2008;283:28873–80.
[12] Jacob C, Holme AL, Fry FH. The sulfinic acid switch in proteins. Org Biomol Chem 2004;2:1953–6.
[13] Lin ST, Chou HC, Chang SJ, Chen YW, Lyu PC, Wang WC, et al. Proteomic analysis of proteins responsible for the development of doxorubicin resistance in human uterine cancer cells. J Proteomics 2012;75:5822–47.
[14] Chen YH, Chou HC, Lin ST, Chen YW, Lo YW, Chan HL. Effect of high glucose on secreted proteome in cultured retinal pigmented epithelium cells: its possible relevance to clinical diabetic retinopathy. J Proteomics 2012;77:111–28.
[15] Chen CP, Chen YH, Chern SR, Chang SJ, Tsai TL, Li SH, et al. Placenta proteome analysis from Down syndrome pregnancies for biomarker discovery. Mol Biosyst 2012;8:2360–72.
[16] Lai TC, Chou HC, Chen YW, Lee TR, Chan HT, Shen HH, et al. Secretomic and proteomic analysis of potential breast cancer markers by two-dimensional differential gel electrophoresis. J Proteome Res 2010;9:1302–22.
[17] Hung PH, Chen YW, Cheng KC, Chou HC, Lyu PC, Lu YC, et al. Plasma proteomic analysis of the critical limb ischemia markers in diabetic patients with hemodialysis. Mol Biosyst 2011;7:1990–8.
[18] Huang HL, Hsing HW, Lai TC, Chen YW, Lee TR, Chan HT, et al. Trypsin-induced proteome alteration during cell subculture in mammalian cells. J Biomed Sci 2010;17:36.
[19] Lai TC, Chou HC, Chen YW, Lee TR, Chan HT, Shen HH, et al. Secretomic and proteomic analysis of potential breast cancer markers by Two-dimensional differential gel electrophoresis. J Proteome Res 2010;9:1302–22.
[20] Chen YW, Chou HC, Lyu PC, Yin HS, Huang FL, Chang WS, et al. Mitochondrial proteomics analysis of tumorigenic and metastatic breast cancer markers. Funct Integr Genomics 2011;11:225–39.

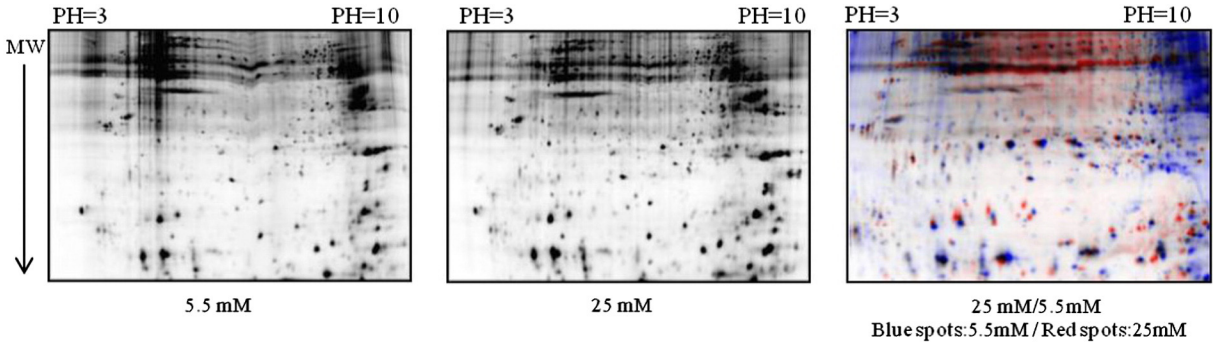

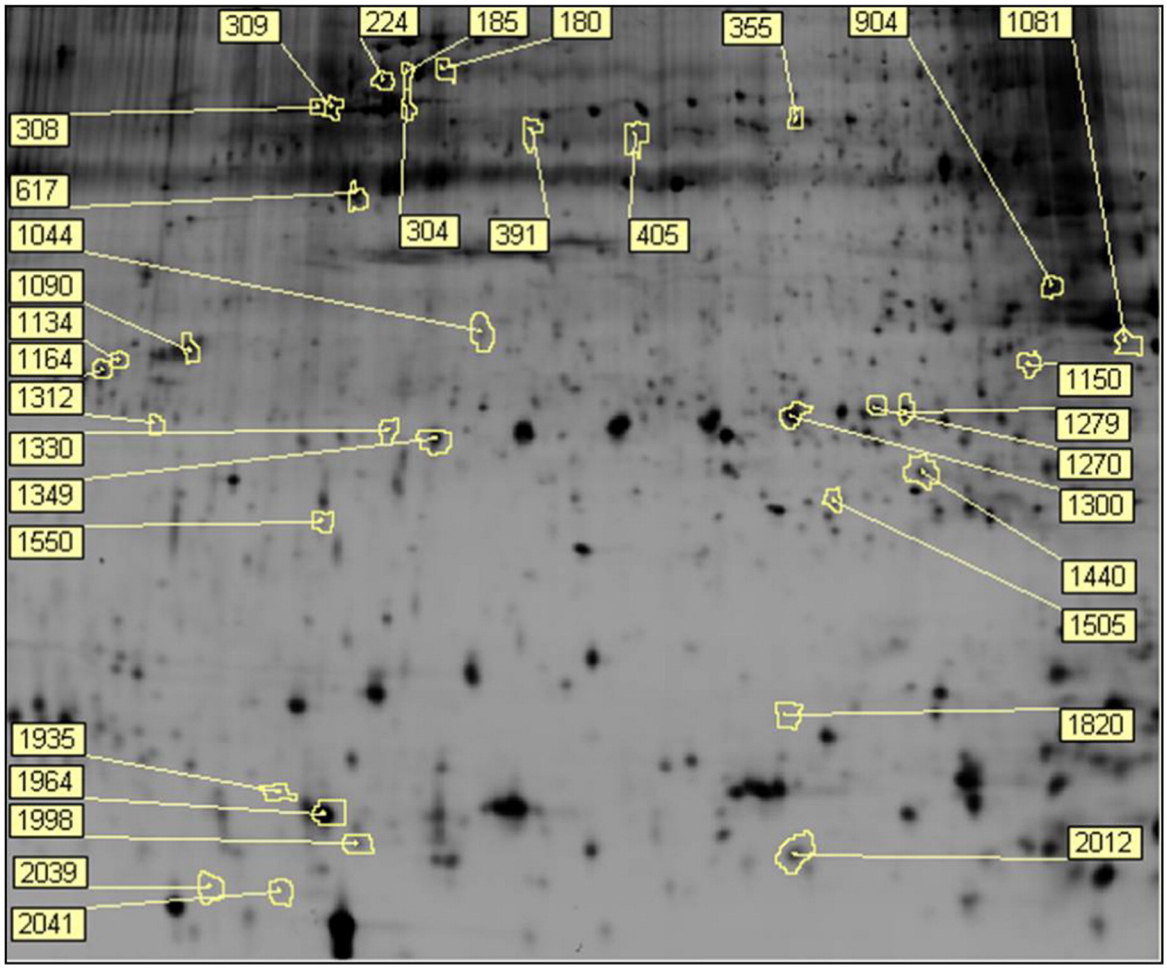

Fig. 9. Redox 2D-DIGE analysis of high glucose-induced differential cysteine-modification in Chang liver cells. Lysates from Chang liver cells cultured in 5.5 mM and 25 mM glucose for at least 3 weeks were subjected to redox 2D-DIGE analysis as described in Materials and Methods. 2-DE-proteome map of Chang liver cultured in mannitol-balanced 5.5 mM and 25 mM glucose are displayed. The differentially labeled protein features are annotated with spot numbers.

[21] Chou HC, Chen YW, Lee TR, Wu FS, Chan HT, Lyu PC, et al. Proteomics study of oxidative stress and Src kinase inhibition in H9C2 cardiomyocytes: A cell model of heart ischemia reperfusion injury and treatment. Free Radic Biol Med 2010;49:96–108.
[22] Chou HC, Lu YC, Cheng CS, Chen YW, Lyu PC, Lin CW, et al. Proteomic and redox-proteomic analysis of berberine-induced cytotoxicity in breast cancer cells. J Proteomics 2012;75:3158–76.
[23] Wu CL, Chou HC, Cheng CS, Li JM, Lin ST, Chen YW, et al. Proteomic analysis of UVB-induced protein expression- and redox-dependent changes in skin fibroblasts using lysine- and cysteine-labeling two-dimensional difference gel electrophoresis. J Proteomics 2012;75:1991–2014.
[24] Chan HL, Gharbi S, Gaffney PR, Cramer R, Waterfield MD, Timms JF. Proteomic analysis of redox- and ErbB2-dependent changes in mammary luminal epithelial cells using cysteine- and lysine-labelling two-dimensional difference gel electrophoresis. Proteomics 2005;5:2908–26.
[25] Lin ST, Chou HC, Chen YW, Chan HL. Redox-proteomic analysis of doxorubicin-induced altered thiol activity in cardiomyocytes. Mol Biosyst 2013;9:447–56.
[26] Lee YR, Chen YW, Tsai MC, Chou HC, Chan HL. Redox- and expression-proteomic analysis of plasma biomarkers in bladder transitional cell carcinoma. Mol Biosyst 2012;8:3314–24.
[27] Chen CC, Lu YC, Chen YW, Lee WL, Lu CH, Chen YH, et al. Hemopexin is up-regulated in plasma from type 1 diabetes mellitus patients: Role of glucose-induced ROS. J Proteomics 2012;75:3760–77.
[28] Chou HC, Lu YC, Cheng CS, Chen YW, Lyu PC, Lin CW, et al. Proteomic and redox-proteomic analysis of berberine-induced cytotoxicity in breast cancer cells. J Proteomics 2012;75:3158–76.
[29] Wu CL, Chou HC, Cheng CS, Li JM, Lin ST, Chen YW, et al. Proteomic analysis of UVB-induced protein expression- and redox-dependent changes in skin fibroblasts using lysine- and cysteine-labeling two-dimensional difference gel electrophoresis. J Proteomics 2012;75:1991–2014.
[30] Candiloros H, Muller S, Zeghari N, Donner M, Drouin P, Ziegler O. Decreased erythrocyte membrane fluidity in poorly controlled IDDM. Influence of ketone bodies. Diabetes Care 1995;18:549–51.

Table 2
Differential cysteine labeled proteins identified by ICy 2D-DIGE and MALDI-TOF MS

No.	Swiss-prot no.	Protein name	pI	MW	No. Match. Peptides	Coverage (%)	Score	Functional classification	Subcellular location	25 mM/5.5 M (Cys/Lys) [a]
300	P10809	60 kDa heat shock protein	5.70	61187	8/18	15	72/56	Protein folding	Mitochondrion-2.11	
654	Q96HG5	Actin, cytoplasmic 1	5.29	42052	5/14	16	70/56	Cytoskeleton	Cytoplasm	−8.33
2003	Q08AH3	Acyl-coenzyme A synthetase	8.34	64809	4/8	7	57/56	Lipid biosynthesis	Mitochondrion	−1.51
754	Q6GMP2	Alpha-enolase	7.01	47481	8/19	15	70/56	Glycolysis	Cytoplasm	−2.18
356	Q9H3R1	Bifunctional heparan sulfate Ndeacetylase/N-sulfotransferase 4	7.19	101222	4/6	5	58/56	Glycoprotein biosynthesis	Golgi	−1.74
452	Q96T60	Bifunctional polynucleotide phosphatase/kinase	8.73	57554	5/12	8	63/56	DNA repair	Nucleus	1.7
818	P61925	cAMP-dependent protein kinase inhibitor alpha	4.45	7984	3/8	44	58/56	PKA inhibitor	Cytoplasm	7.89
1953	P23528	Cofilin-1	8.22	18719	7/15	45	81/56	Cytoskeleton regulation	Nucleus	−2.39
1995	P62937	cyclophilin A	7.68	18229	6/18	36	84/56	Protein folding	Cytoplasm	−1.57
44	Q96AE4	DNA helicase V / Far upstream element-binding protein 1	7.18	67690	9/22	14	70/56	Gene regulation	Nucleus	1.79
302	Q96AE4	DNA helicase V / Far upstream element-binding protein 1	7.18	67690	8/29	17	90/56	Gene regulation	Nucleus	−1.53
174	P04062	Glucosylceramidase	7.29	60134	5/11	13	62/56	Lipid catabolism	Lysosome	1.86
111	P08107	Heat shock 70 kDa protein	5.48	70294	9/17	19	68/56	Protein folding	Cytoplasm	1.58
1646	Q9UC36	Heat shock protein beta-1	5.98	22826	6/16	28	62/56	Protein folding	Cytoplasm	17.14
1088	P51991	Heterogeneous nuclear ribonucleoprotein A3	9.10	39799	6/14	23	76/56	Gene regulation	Nucleus	1.72
790	O75610	Left-right determination factor B	8.60	41367	6/12	17	56/56	Cell growth	Secreted	−1.6
1687	Q06830	Peroxiredoxin-1	8.27	22324	8/22	45	94/56	Redox regulation	Cytoplasm	2.28
608	P00558	Phosphoglycerate kinase 1	8.30	44985	10/17	28	81/56	Glycolysis	Cytoplasm	−1.58
942	Q9Y2S7	Polymerase delta-interacting protein 2	8.80	42235	7/19	19	56/56	DNA replication	Nucleus	6.49
1072	Q9Y2S7	Polymerase delta-interacting protein 2	8.80	42235	7/19	19	56/56	DNA replication	Nucleus	1.92
749	P61019	Ras-related protein Rab-2A	6.08	23702	5/10	18	70/56	Protein trafficking	ER	−1.63
1385	O94989	Rho guanine nucleotide exchange factor 15	9.61	92852	10/16	10	67/56	GTPase activation	Cytoplasm	2.20
1326	Q8IXI3	Serpin B3	6.35	44594	7/11	16	68/56	Protease inhibitor	Cytoplasm	−9.48
1233	O75937	Splicing protein spf31	9.04	29823	6/9	20	58/56	Gene regulation	Nucleus	1.77
1286	O75937	Splicing protein spf31	9.04	29823	6/9	20	56/58	Gene regulation	Nucleus	1.61
782	P01730	T-cell surface glycoprotein CD4	9.60	51705	6/8	12	60/56	Immuno response	Plasma membrane	−2.46
1334	Q9NVH6	Trimethyllysine dioxygenase	7.64	50113	6/11	13	58/56	Redox regulation	Mitochondrion	−5.63
193	Q70CQ4	Ubiquitin carboxyl-terminal hydrolase	9.35	148328	9/10	4	60/56	Protein degradation	Cytoplasm	1.83
462	P11172	Uridine 5′-monophosphate synthase	6.81	52645	5/8	11	64/56	Pyrimidine biosynthesis	Cytoplasm	−1.61

Proteins displaying high glucose-induced differential labeling of cysteines using ICy dyes were identified by MALDI-TOF peptide mass mapping analysis. Proteins with thiol reactivity displaying an average fold-difference of ≥1.3-fold where $P<.05$ and spots matched in all images are listed in this table.

[a] Average fold differences of triplicate samples run on different gels from DeCyder analysis show labeling changes on free thiol group of cysteine residues for Chang liver cells maintained in 25 mM glucose *versus* in 5.5 mM glucose. In here, ICy5 signals were used to monitor cysteine-labeling alterations against ICy3 signals used as internal standard followed by normalized with protein expression changes. NHS-Cy2 was used to label lysine residues on proteins (to monitor protein expression changes) and was used to normalize ICy3 signals used as internal standard.

[31] Saydah SH, Miret M, Sung J, Varas C, Gause D, Brancati FL. Postchallenge hyperglycemia and mortality in a national sample of U.S. adults. Diabetes Care 2001;24:1397–402.
[32] Jouven X, Lemaitre RN, Rea TD, Sotoodehnia N, Empana JP, Siscovick DS. Diabetes, glucose level, and risk of sudden cardiac death. Eur Heart J 2005;26:2142–7.
[33] Cai L, Li W, Wang G, Guo L, Jiang Y, Kang YJ. Hyperglycemia-induced apoptosis in mouse myocardium: mitochondrial cytochrome C-mediated caspase-3 activation pathway. Diabetes 2002;51:1938–48.
[34] Chan HL, Gharbi S, Gaffney PR, Cramer R, Waterfield MD, Timms JF. Proteomic analysis of redox- and ErbB2-dependent changes in mammary luminal epithelial cells using cysteine- and lysine-labelling two-dimensional difference gel electrophoresis. Proteomics 2005;5:2908–26.
[35] Gharbi S, Gaffney P, Yang A, Zvelebil MJ, Cramer R, Waterfield MD, et al. Evaluation of two-dimensional differential gel electrophoresis for proteomic expression analysis of a model breast cancer cell system. Mol Cell Proteomics 2002;1:91–8.
[36] Lin CP, Chen YW, Liu WH, Chou HC, Chang YP, Lin ST, et al. Proteomic identification of plasma biomarkers in uterine leiomyoma. Mol Biosyst 2011;8:1136–45.
[37] Chen YW, Liu JY, Lin ST, Li JM, Huang SH, Chen JY, et al. Proteomic analysis of gemcitabine-induced drug resistance in pancreatic cancer cells. Mol Biosyst 2011;7:3065–74.
[38] Ghezzi P, Bonetto V, Fratelli M. Thiol-disulfide balance: from the concept of oxidative stress to that of redox regulation. Antioxid Redox Signal 2005;7:964–72.
[39] Rohde M, Daugaard M, Jensen MH, Helin K, Nylandsted J, Jaattela M. Members of the heat-shock protein 70 family promote cancer cell growth by distinct mechanisms. Genes Dev 2005;19:570–82.
[40] Ramachandran S, Venugopal A, Sathisha K, Reshmi G, Charles S, Divya G, et al. Proteomic profiling of high glucose primed monocytes identifies cyclophilin A as a potential secretory marker of inflammation in type 2 diabetes. Proteomics 2012;12:2808–21.
[41] Wilson CH, Zeile S, Chataway T, Nieuwenhuijs VB, Padbury RT, Barritt GJ. Increased expression of peroxiredoxin 1 and identification of a novel lipid-metabolizing enzyme in the early phase of liver ischemia reperfusion injury. Proteomics 2011;11:4385–96.
[42] Mori K. Cellular response to endoplasmic reticulum stress mediated by unfolded protein response pathway. Tanpakushitsu Kakusan Koso 1999;44:2442–8.
[43] Sadighi Akha AA, Harper JM, Salmon AB, Schroeder BA, Tyra HM, Rutkowski DT, et al. Heightened induction of proapoptotic signals in response to endoplasmic reticulum stress in primary fibroblasts from a mouse model of longevity. J Biol Chem 2011;286:30344–51.
[44] Kitiphongspattana K, Mathews CE, Leiter EH, Gaskins HR. Proteasome inhibition alters glucose-stimulated (pro)insulin secretion and turnover in pancreatic {beta}-cells. J Biol Chem 2005;280:15727–34.
[45] Nakamura K, Bossy-Wetzel E, Burns K, Fadel MP, Lozyk M, Goping IS, et al. Changes in endoplasmic reticulum luminal environment affect cell sensitivity to apoptosis. J Cell Biol 2000;150:731–40.
[46] Akita Y. Protein kinase C-epsilon (PKC-epsilon): its unique structure and function. J Biochem 2002;132:847–52.
[47] Naor Z, Shacham S, Harris D, Seger R, Reiss N. Signal transduction of the gonadotropin releasing hormone (GnRH) receptor: cross-talk of calcium, protein kinase C (PKC), and arachidonic acid. Cell Mol Neurobiol 1995;15:527–44.

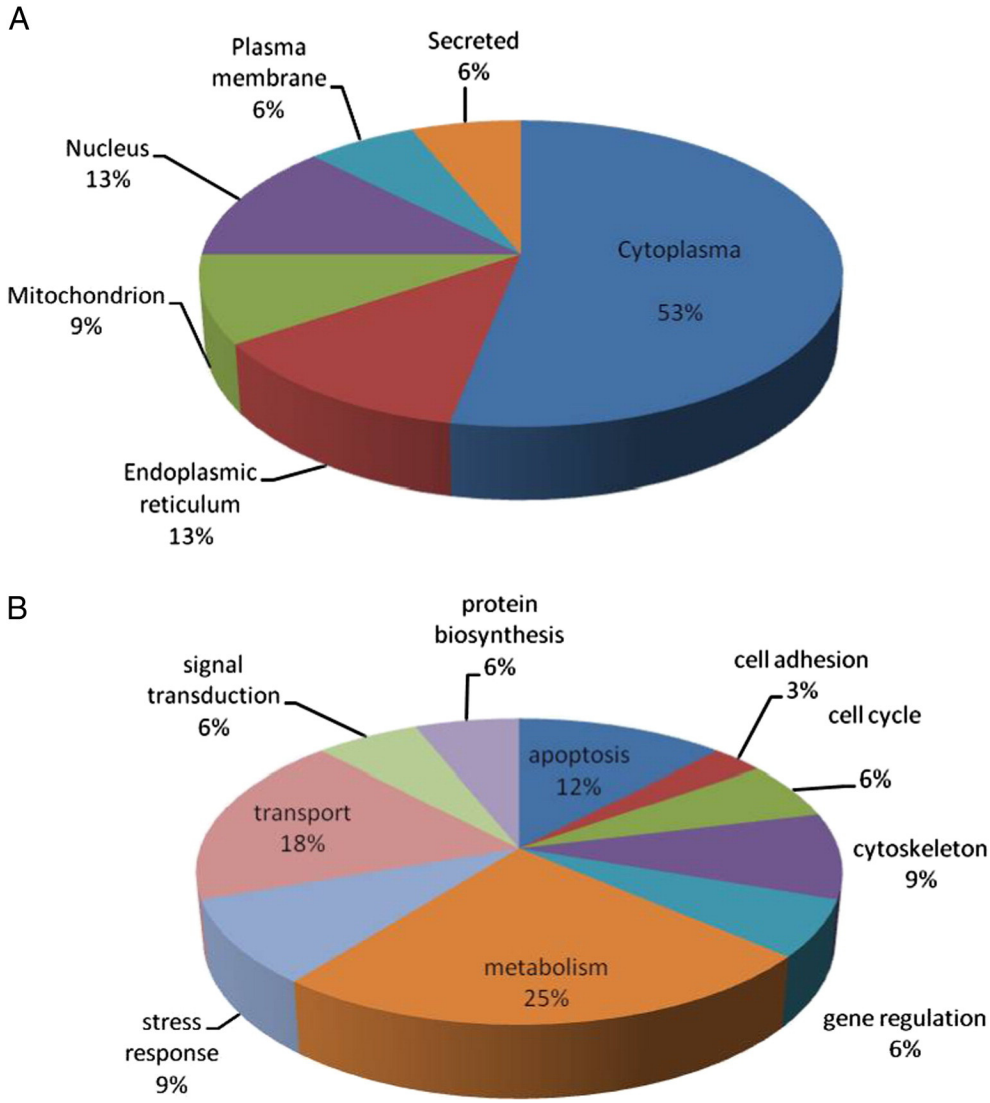

Fig. 10. Distribution of differential ICy-labeled proteins between 25 mM glucose and 5.5 mM glucose incubated Chang liver cells according to (A) subcellular location and (B) biological function. The classification of the biological functions and sub-cellular locations of these identified proteins are based on a Swiss-Prot search and KEGG pathway analysis.

[48] Allenby G, Bocquel MT, Saunders M, Kazmer S, Speck J, Rosenberger M, et al. Retinoic acid receptors and retinoid X receptors: interactions with endogenous retinoic acids. Proc Natl Acad Sci U S A 1993;90:30–4.
[49] Singh AB, Guleria RS, Nizamutdinova IT, Baker KM, Pan J. High glucose-induced repression of RAR/RXR in cardiomyocytes is mediated through oxidative stress/JNK signaling. J Cell Physiol 2011;227:2632–44.
[50] Guleria RS, Choudhary R, Tanaka T, Baker KM, Pan J. Retinoic acid receptor-mediated signaling protects cardiomyocytes from hyperglycemia induced apoptosis: role of the renin-angiotensin system. J Cell Physiol 2011;226:1292–307.
[51] Mori M, Metzger D, Picaud S, Hindelang C, Simonutti M, Sahel J, et al. Retinal dystrophy resulting from ablation of RXR alpha in the mouse retinal pigment epithelium. Am J Pathol 2004;164:701–10.

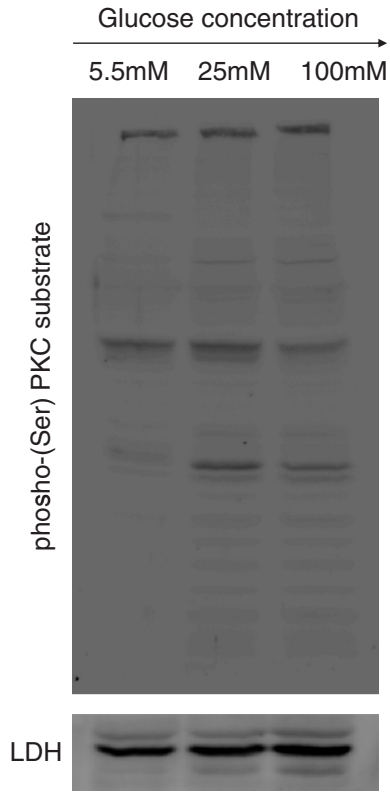

Fig. 11. Immunoblotting analysis the activation of Phospho-(Ser) PKC substrates for Chang liver cells incubated in 5.5 mM, 25 mM and 100 mM glucose. Chang liver cells incubated in 5.5 mM, 25 mM and 100 mM glucose for at least 3 weeks and immunoblotted with anti-Phospho-(Ser) PKC substrates antibody.